iScience

CellPress
OPEN ACCESS

Article

RHOF activation of AKT/β-catenin signaling pathway drives acute myeloid leukemia progression and chemotherapy resistance

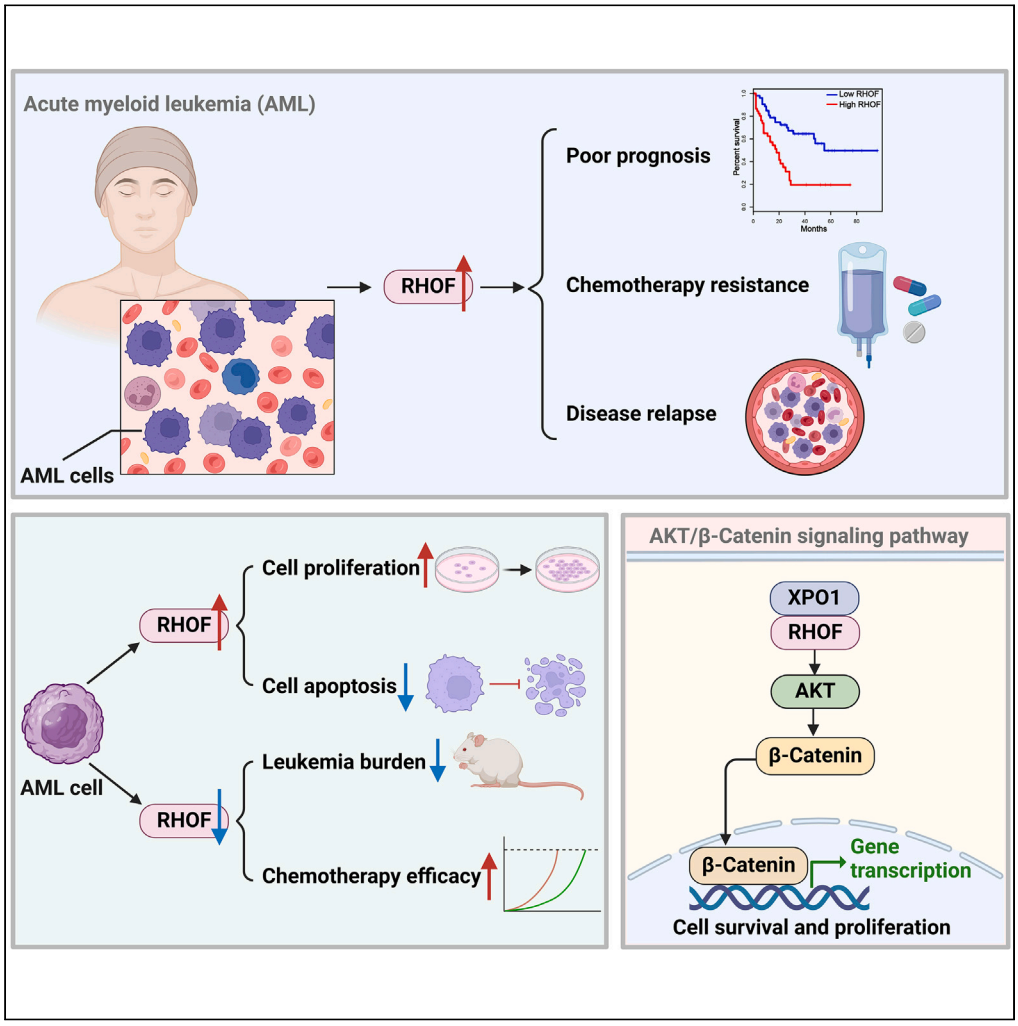

Xin Wen, Peng Li, Yuechan Ma, ..., Fei Lu, Jingjing Ye, Chunyan Ji

lufeisdu2@163.com (F.L.)
jichunyan@sdu.edu.cn (C.J.)

Highlights

High RHOF expression in AML predicts poor prognosis

RHOF promotes AML proliferation through AKT/β-catenin signaling pathway

XPO1 interacts with RHOF and regulates RHOF expression in AML

RHOF inhibition offers a promising strategy in AML treatment

Wen et al., iScience 27, 110221
July 19, 2024
https://doi.org/10.1016/j.isci.2024.110221

iScience

CellPress
OPEN ACCESS

Article

RHOF activation of AKT/β-catenin signaling pathway drives acute myeloid leukemia progression and chemotherapy resistance

Xin Wen,[1,3] Peng Li,[1,3] Yuechan Ma,[1] Dongmei Wang,[2] Ruinan Jia,[1] Yuan Xia,[1] Wei Li,[1] Yongjian Li,[1] Guosheng Li,[1,2] Tao Sun,[1,2] Fei Lu,[1,*] Jingjing Ye,[1,2] and Chunyan Ji[1,2,4,*]

SUMMARY

Acute myeloid leukemia (AML) is a clonal malignancy originating from leukemia stem cells, characterized by a poor prognosis, underscoring the necessity for novel therapeutic targets and treatment methodologies. This study focuses on Ras homolog family member F, filopodia associated (RHOF), a Rho guanosine triphosphatase (GTPase) family member. We found that RHOF is overexpressed in AML, correlating with an adverse prognosis. Our gain- and loss-of-function experiments revealed that RHOF overexpression enhances proliferation and impedes apoptosis in AML cells *in vitro*. Conversely, genetic suppression of RHOF markedly reduced the leukemia burden in a human AML xenograft mouse model. Furthermore, we investigated the synergistic effect of RHOF downregulation and chemotherapy, demonstrating significant therapeutic efficacy *in vivo*. Mechanistically, RHOF activates the AKT/β-catenin signaling pathway, thereby accelerating the progression of AML. Our findings elucidate the pivotal role of RHOF in AML pathogenesis and propose RHOF inhibition as a promising therapeutic approach for AML management.

INTRODUCTION

Acute myeloid leukemia (AML), a clonal hematologic malignancy, is characterized by the unchecked proliferation of immature hematopoietic cells. This overgrowth not only disrupts normal hematopoiesis but also leads to the infiltration of AML cells into various organs, critically impairing overall health.[1] Despite advancements in therapeutic strategies, including combination chemotherapy, hematopoietic stem cell transplantation, and targeted gene therapy, the treatment of AML remains a formidable challenge. While these treatments have improved the complete remission (CR) rates and extended five-year disease-free survival, a significant proportion of AML patients experiences relapse after achieving CR. Moreover, some patients develop refractory leukemia, which is resistant to combination chemotherapy, resulting in a dire prognosis.[2] The etiology of AML is multifactorial, encompassing gene mutations, aberrant signaling pathways, epigenetic alterations, an altered leukemic microenvironment, and immune system imbalances.[3–5] Therefore, further understanding of the molecular mechanisms involved in AML occurrence and development and identifying therapeutic targets for patients with AML are important.

Among potential targets, Rho GTPases, a subgroup of the Ras GTPase superfamily, have garnered significant attention. These GTPases, which are activated by Rho guanine nucleotide exchange factors at cellular membranes, play pivotal roles in various biological processes.[6,7] The Rho GTPase family, which includes 20 members across eight subfamilies, is instrumental in mediating cellular functions such as vesicle translocation and cytoskeletal rearrangement.[8–10] In cancer biology, Rho GTPases are increasingly recognized for their correlation with tumor progression and poor prognosis.[11–22] They are integral to hematopoiesis, influencing cell proliferation, differentiation, migration, and self-renewal.[23–28]

A specific focus of our study was RHOF, a member of the GTPase family, known for its involvement in numerous cellular processes, including filopodium remodeling, axonogenesis, and cell adhesion.[7,29,30] RHOF induces filopodia through mDia2, playing a critical role in cytoskeletal reorganization and membrane trafficking as a master regulator.[31,32] Elevated RHOF expression has been implicated in poor prognosis in various cancers, such as pancreatic cancer, hepatocellular carcinoma, and breast cancer, due to its roles in processes such as epithelial-mesenchymal transition and NF-κB activation.[33–37] However, the exact role of RHOF in AML and its contribution to the molecular pathogenesis of this disease remain underexplored.

Our study aimed to comprehensively analyze the association between RHOF expression and AML, leveraging both clinical data and experimental models. We examined RHOF expression in AML patients through in-depth clinical analysis and probed its oncogenic potential in AML using *in vitro* and *in vivo* experiments. Our findings revealed a strong correlation between elevated RHOF expression and increased

[1]Department of Hematology, Qilu Hospital, Cheeloo College of Medicine, Shandong University, Jinan 250012, People's Republic of China
[2]Shandong Key Laboratory of Immunohematology, Qilu Hospital, Shandong University, Jinan 250012, People's Republic of China
[3]These authors contributed equally
[4]Lead contact
*Correspondence: lufeisdu2@163.com (F.L.), jichunyan@sdu.edu.cn (C.J.)
https://doi.org/10.1016/j.isci.2024.110221

proliferation of AML cells. This effect is predominantly mediated through the AKT/β-catenin signaling pathway. Notably, our study revealed that RHOF is a key mediator of AML resistance to frontline chemotherapy drugs. By targeting RHOF, we propose an approach to enhance the sensitivity of AML cells to chemotherapy, potentially improving the effectiveness of current treatments. Our research thus elucidates the critical role of RHOF in AML progression, offers insights into the pathophysiology of this complex disease and opens avenues for targeted therapeutic interventions.

RESULTS

AML exhibits high levels of RHOF expression

We initially utilized the The Cancer Genome Atlas (TCGA) database to examine the expression of RHOF in AML, with the aim of revealing its diagnostic and therapeutic potential. Our analysis revealed a marked increase in *RHOF* expression levels in AML patients compared to normal bone marrow controls (Figure 1A). This distinction underscores the potential role of RHOF in the pathogenesis of AML. Further analysis leveraging data from the BloodSpot database (https://www.bloodspot.eu) revealed pronounced *RHOF* expression in AML patients with complex karyotypes (Figure 1B). This finding is particularly intriguing, as it suggests a possible link between *RHOF* expression and genetic complexity in AML.

Our subsequent survival analysis, using the GEPIA2 web server revealed a significant association between high *RHOF* expression and poorer patient outcomes in patients with AML (Figure 1C). This correlation indicates a strong negative impact of *RHOF* expression on the prognosis of AML patients. In addition, we observed a significant increase in RHOF protein expression in AML patients compared to that in patients who achieved CR (Figure 1D). Furthermore, we examined mononuclear cells extracted from the bone marrow of three patient groups: newly diagnosed (ND) AML patients, patients with relapsed/refractory (RR) AML, and patients in CR. A summary of the clinical characteristics is provided in Table S1. A striking increase in *RHOF* mRNA expression was observed in the ND ($n = 31$, $p < 0.001$) and RR ($n = 25$, $p < 0.0001$) groups compared with the CR group ($n = 20$, Figure 1E). Notably, *RHOF* levels were highest in patients with RR AML, suggesting that RHOF is involved in disease relapse and refractoriness (ND vs. RR, $p < 0.05$, Figure 1E). Furthermore, RHOF expression was significantly higher in $CD34^+$ AML cells than in $CD34^-$ cells from ND AML patients, confirming that the high levels of RHOF observed in the bone marrow cells of AML patients are predominantly due to the AML cells themselves (Figure 1F).

This observation was further substantiated by our examination of leukemia cell lines. Both the THP-1 and MOLM-13 AML cell lines showed a considerable increase in RHOF expression at the mRNA and protein levels compared to that in human bone marrow stromal HS-5 cells (Figures 1G and 1H). These collective findings highlight the global upregulation of RHOF in AML, suggesting that RHOF is a crucial molecular player in the pathology and progression of this disease. This upregulation not only correlates with poorer clinical outcomes but also indicates a significant role of RHOF in the complex genomic landscape of AML.

Cell growth is inhibited, and apoptosis and chemotherapeutic drug-induced apoptosis are enhanced through the suppression of RHOF

To determine the critical role of RHOF suppression in the survival of AML cells, we used short hairpin RNA (shRNA) to decrease RHOF expression in the THP-1 and MOLM-13 AML cell lines. As shown in Figure 2A, a reduction in RHOF expression was confirmed at both the mRNA and protein levels through RT-qPCR and western blotting. After successful suppression of RHOF expression, we assessed its impact on AML cell growth using the Cell Counting Kit-8 (CCK-8) assay. As shown in Figure 2B, the inhibition of RHOF led to a significant reduction in AML cell proliferation. This observation was further supported by the assessment of the colony formation ability of the AML cells (Figure 2C). The results provided additional evidence that the reduction in RHOF markedly impaired the ability of the cells to form colonies, thus emphasizing the inhibitory role of RHOF suppression in cell proliferation. Moreover, we investigated cell apoptosis, as illustrated in Figure 2D. Notably, the reduction in RHOF expression was associated with a marked increase in cell apoptosis. These findings underscore the role of RHOF as an essential factor for AML cell survival. In a more clinically relevant context, we explored the potential implications of reduced RHOF expression in the area of AML treatment. We observed that when RHOF was knocked down in THP-1 and MOLM-13 AML cells and subsequently subjected to treatment with Ara-C and idarubicin (IDA), there was a substantial increase in apoptosis (Figure 2E). These findings suggested that reducing RHOF expression can augment the chemosensitivity of AML cells, potentially increasing their responsiveness to therapeutic interventions.

RHOF depletion markedly reduces the leukemia load in human AML xenografts

Subsequently, we investigated the importance of RHOF *in vivo* using a mouse model of xenotransplantation. NSG mice were injected intravenously with either reduced RHOF-expressing or control THP-1 cells. The mice were regularly monitored for leukemia progression. To evaluate the burden of leukemia, the infiltration of AML cells and the degree of organ enlargement were evaluated. Thirty-six days after receiving an intravenous injection, both groups exhibited signs of disease onset and progression, such as body weight loss and reduced body condition (Figure 3A). To visualize AML cells in mice, we engineered THP-1 leukemia cells to express GFP as a marker. We then used the fluorescence intensity of GFP, detected by an animal imaging system, to monitor the distribution of AML cells within the mice. According to the *in vivo* findings, a significantly lower percentage of AML cells in the RHOF knockdown groups than in the control group were detected by pseudocolor fluorescence intensity imaging system (Figure 3B). In mice injected with RHOF-knockdown cells, splenomegaly was ameliorated (Figure 3C), and the amount of leukemic infiltration in the liver was markedly reduced (Figure 3D). Flow cytometry confirmed that reducing RHOF

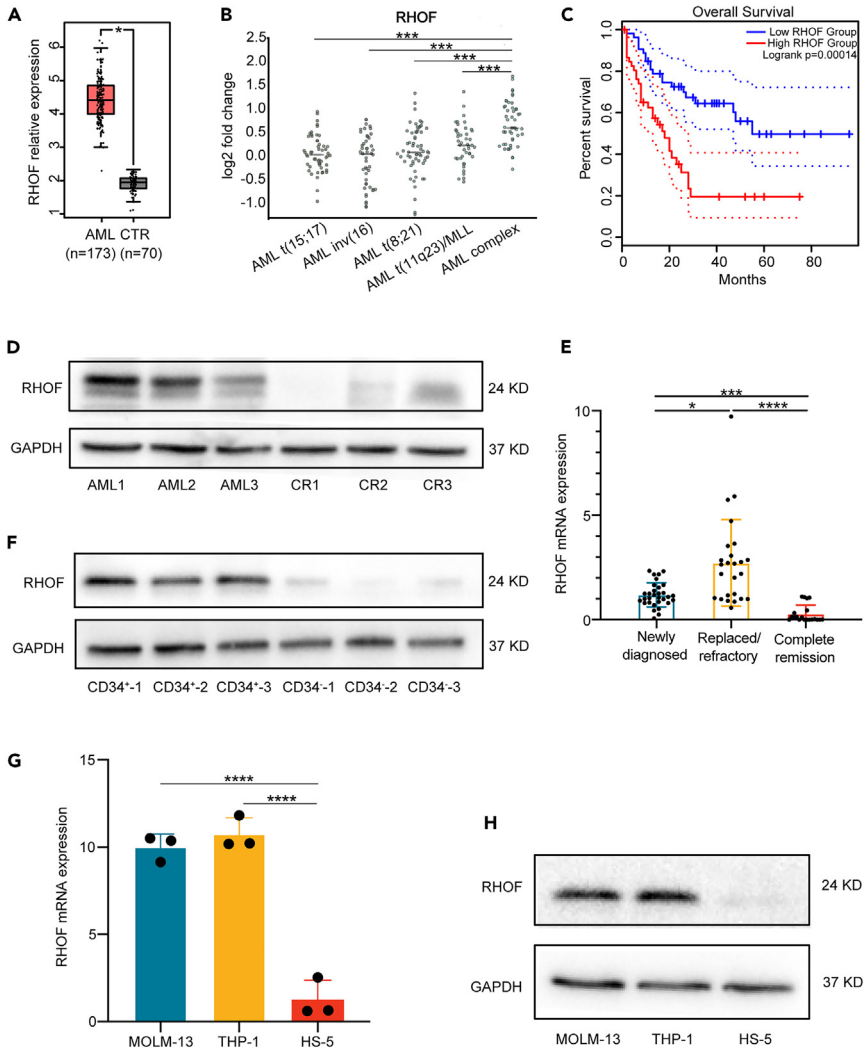

Figure 1. AML exhibits high levels of RHOF expression

(A) *RHOF* expression was measured in 173 AML samples (red) and 70 control samples (gray) utilizing data from the GEPIA2 database.

(B) *RHOF* expression levels in patients with complex karyotypes.

(C) OS comparison between the high-RHOF (n = 53) and low-RHOF (n = 53) groups in the TCGA database analyzed via the GEPIA web server.

(D) RHOF in patients with newly diagnosed AML and CR AML patients determined by western blot analysis.

(E) *RHOF* mRNA expression levels in newly diagnosed AML patients (n = 31), relapsed/refractory AML patients (n = 25), and complete remission AML patients (n = 20) were analyzed via RT-qPCR. The nonparametric Kruskal-Walli test was used.

(F) RHOF expression in $CD34^+$ cells compared to that in $CD34^-$ cells from ND AML patients, as determined by western blot analysis.

(G) *RHOF* expression in THP-1 and MOLM-13 cells relative to that in HS-5 cells determined by RT-qPCR analysis (n = 3).

(H) Western blot analysis was used to compare the protein expression levels of RHOF in THP-1 and MOLM-13 cells with those in HS-5 cells. Student's t test was utilized to analyze differences between two groups. One-way ANOVA test was used for multiple variable comparison. Survival analyses were performed with the log rank test. The data are presented as the means ± SD. *$p < 0.05$; **$p < 0.01$; ***$p < 0.001$.

expression resulted in a notable reduction in human leukemia cells ($CD45^+$) in the bone marrow, peripheral blood, spleen, and liver (Figure 3E). As shown in Figure 3F, the shRHOF AML mice exhibited reduced leukemic infiltration in their bone marrow, spleen, and liver. This observation was confirmed through immunofluorescence staining. Additionally, our results showed that shRHOF prolonged the survival time of the mice (Figure 3G). Overall, these findings demonstrated that RHOF plays a vital role in AML initiation and progression.

RHOF overexpression promotes cell growth and prevents chemotherapeutic-induced apoptosis

To further determine the critical role of elevated RHOF expression in regulating cellular proliferation and the reaction to chemical intervention, we used an RHOF-expressing lentivirus to overexpress RHOF in the THP-1 and MOLM-13 AML cell lines. As shown in Figure 4A, the

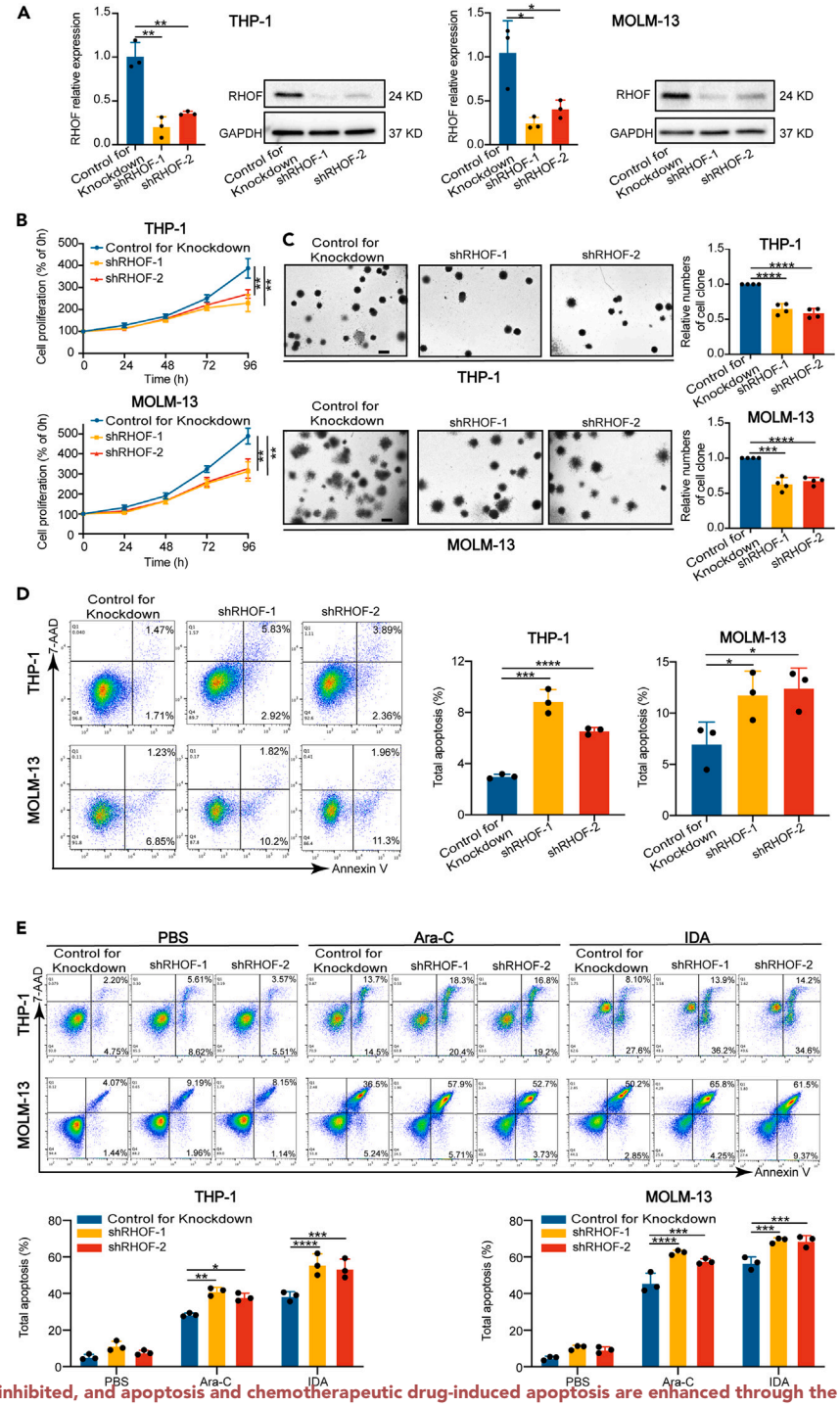

Figure 2. Cell growth is inhibited, and apoptosis and chemotherapeutic drug-induced apoptosis are enhanced through the suppression of RHOF

(A) Puromycin-selected RHOF-knockdown (shRHOF) or nonsilencing scrambled control (control for knockdown) THP-1 and MOLM-13 cells were subjected to RT-qPCR (n = 3) and western blotting.

(B) Proliferation of control for knockdown or shRHOF cells was determined by CCK-8 assays at 0, 24, 48, 72, and 96 h (n = 4).

(C) Colony formation assays (left). Scale bar: 500 μm. The statistical analysis is shown in the right panel (n = 4).

(D) Apoptosis analysis of THP-1 and MOLM-13 (control for knockdown or shRHOF) cells was performed via flow cytometry (n = 3).

(E) THP-1 and MOLM-13 cells (control for knockdown or shRHOF) were treated with 1.2 μM Ara-C and 0.03 μg/mL IDA for 48 h to measure apoptosis via flow cytometry (n = 3). Student's t tests were used for comparing two variables. One-way ANOVA test was used for multiple variable comparison. The means ± SD are shown. *$p < 0.05$; **$p < 0.01$; ***$p < 0.001$.

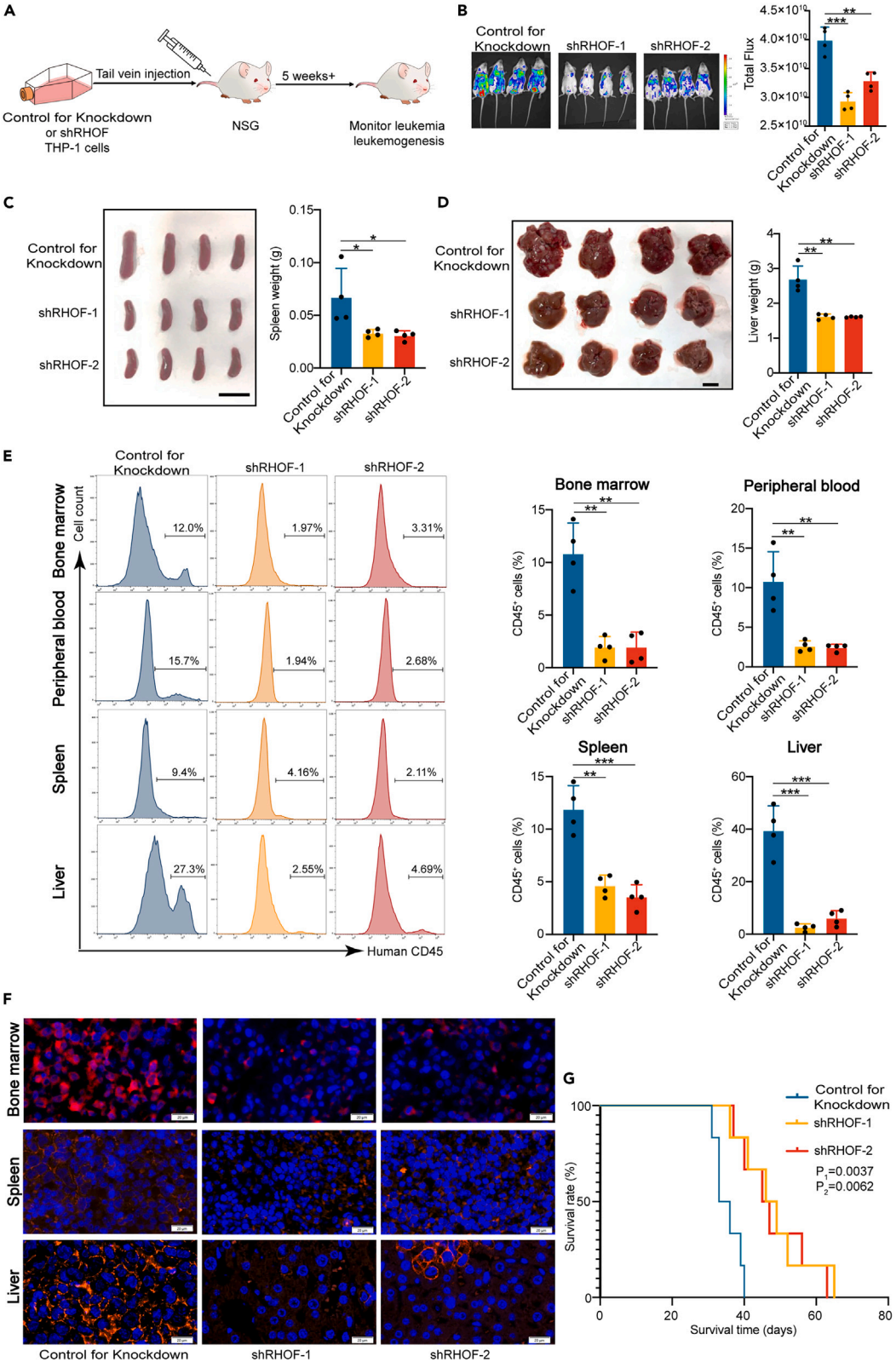
A
Tail vein injection
5 weeks+
Control for Knockdown or shRHOF THP-1 cells
NSG
Monitor leukemia leukemogenesis
B
Control for Knockdown
shRHOF-1
shRHOF-2
Total Flux
C
Control for Knockdown
shRHOF-1
shRHOF-2
Spleen weight (g)
D
Liver weight (g)
E
Bone marrow
Peripheral blood
Spleen
Liver
Cell count
12.0%
1.97%
3.31%
15.7%
1.94%
2.68%
9.4%
4.16%
2.11%
27.3%
2.55%
4.69%
Human CD45
CD45+ cells (%)
F
G
Survival rate (%)
Survival time (days)
P1=0.0037
P2=0.0062

Figure 3. RHOF depletion markedly reduces the leukemia load in human AML xenografts

(A) Schematic of the xenotransplantation experiment.

(B) Detection of GFP signals *in vivo* using pseudocolor fluorescence intensity in mice transplanted with either control for knockdown or shRHOF THP-1 cells ($n = 4$). The unit of radiance is photons/second/cm^2/steradian.

(C) Representative spleen images and weights of control for knockdown and shRHOF-treated THP-1 cells ($n = 4$). Scale bar: 1 cm.

(D) Representative liver images and weights of control for knockdown and shRHOF-treated THP-1 cells ($n = 4$). Scale bar: 1 cm.

(E) Flow cytometry was used to analyze human CD45$^+$ cells from the bone marrow, peripheral blood, spleen, and liver ($n = 4$).

(F) Immunofluorescence staining of hCD45 in mouse bone marrow, spleen and liver from the three groups. DAPI (blue). hCD45 (red). Scale bar: 20 μm.

(G) The survival rates of mice transplanted with control for knockdown or shRHOF-transduced THP-1 cells ($n = 6$). Student's t tests were used for comparing two variables. K-M survival analyses were performed with the log rank test. The data are presented as the means ± SD. *$p < 0.05$; **$p < 0.01$; ***$p < 0.001$, p1: control for knockdown vs. shRHOF-1, p2: control for knockdown vs. shRHOF-2.

increase in RHOF expression was confirmed at both the mRNA and protein levels through RT-qPCR and western blotting. Additionally, the presence of the FLAG tag results in a slight increase in the molecular weight of the exogenously expressed RHOF compared to that of the endogenous protein. This molecular weight difference is approximately 3 kDa, which is responsible for the appearance of the double band on the western blot. The upper band represents the tagged RHOF, while the lower band corresponds to the native, untagged RHOF expressed by the cells. After successful overexpression of RHOF, we assessed the impact of RHOF on AML cell growth using a CCK-8 assay. As shown in Figure 4B, the upregulation of RHOF led to a significant increase in AML cell proliferation. This observation was further supported by the assessment of the colony formation ability of the AML cells (Figure 4C). The results provided additional evidence that the upregulation of RHOF markedly enhanced the ability of the cells to form colonies, thus emphasizing the role of RHOF in promoting cell proliferation. To analyze our data in a more clinically relevant manner, we explored the potential implications of RHOF overexpression in the area of AML treatment. We observed that when RHOF was overexpressed in THP-1 and MOLM-13 AML cells and subsequently subjected to treatment with Ara-C and IDA, there was a substantial decrease in apoptosis (Figure 4D). This finding suggested that RHOF overexpression can prevent the chemosensitivity of AML cells, potentially increasing their insensitivity to therapeutic interventions. These results collectively support the hypothesis that the upregulation of RHOF plays a crucial role in facilitating AML cell survival, promoting proliferation, and decreasing chemosensitivity.

RHOF augments AML proliferation via the AKT/β-catenin pathway

Our subsequent objective was to pinpoint the fundamental processes responsible for the cancer-causing characteristics facilitated by RHOF. The β-catenin pathway plays a pivotal role in the regulation of AML processes,[38–40] and we speculated that RHOF knockdown induces protein expression changes by influencing β-catenin signaling. To address this possibility, immunofluorescence staining was used to confirm that β-catenin was localized to the nucleus in response to RHOF overexpression (Figure 5A). Furthermore, we measured the protein expression levels of β-catenin by western blotting and showed that β-catenin was decreased in cells in which RHOF was depleted (Figure 5B), suggesting that β-catenin may be a downstream target of RHOF. After observing the impacts of RHOF on the initiation of β-catenin signaling, we investigated the influence of β-catenin on the malignant activities mediated by RHOF. To confirm that β-catenin is responsible for the stimulatory effect of RHOF on AML, rescue experiments were conducted *in vitro*. The CCK-8 assay revealed that the inhibition of β-catenin significantly reversed the promotion of cell proliferation caused by RHOF overexpression (Figure 5C). Similarly, flow cytometry analysis showed that the inhibition of β-catenin significantly reversed the inhibition of cell apoptosis caused by RHOF overexpression (Figure 5D). Interestingly, cells with low RHOF expression and β-catenin agonist promoted cell proliferation compared to shRHOF cells. This finding suggested that the RHOF-mediated modulation of proliferation in AML cells is partially mediated through its effect on β-catenin (Figure S1). To better understand how RHOF affects the β-catenin pathway, we additionally analyzed the level of a crucial upstream regulator, p-AKT, through western blotting, which revealed that a reduction in RHOF led to a decrease in AKT phosphorylation in the cells (Figure 5E). To investigate how AKT contributes to AML progression, an AKT agonist (SC-79) was added to shRHOF-1 THP-1 and MOLM-13 cells, which were found to increase p-AKT and β-catenin levels (Figure 5F). These data indicate that RHOF exerts its protumor effects via activation of the AKT/β-catenin pathway.

RHOF diminishes the responsiveness of AML cells to chemotherapy drugs *in vivo*

We created a mouse model for xenotransplantation to investigate whether RHOF can increase AML chemoresistance *in vivo*. THP-1 cells with RHOF knockdown and control for knockdown cells were injected intravenously into NSG mice. Before chemotherapy, the mice were divided into the following four subgroups: (1) control for knockdown, (2) shRHOF-1, (3) control for knockdown and DA (doxorubicin (DOX) +Ara-C), and (4) shRHOF-1 and DA. On the 30th day after establishing the AML mouse model, the DA regimen was initiated. The regimen involved administering the drugs intraperitoneally to the mice for three consecutive days. Subsequently, Ara-C was administered intraperitoneally on days 33 and 34.

In vivo findings indicated a notable decrease in the ratio of AML cells in the bone marrow and liver in the RHOF knockdown group compared to the control group. RHOF knockdown also reduced the proportion of AML cells observed after chemotherapy (Figures 6A and 6B). Furthermore, in mice, RHOF knockdown in AML cells resulted in significantly reduced spleen and liver sizes after chemotherapy (Figures 6C and 6D). We found that shRHOF-1 and DA significantly inhibited AML cell growth, indicating that synergizing shRHOF treatment with DA may be effective against AML. As shown in Figure 6E, flow cytometry staining confirmed that the burden of human leukemia cells

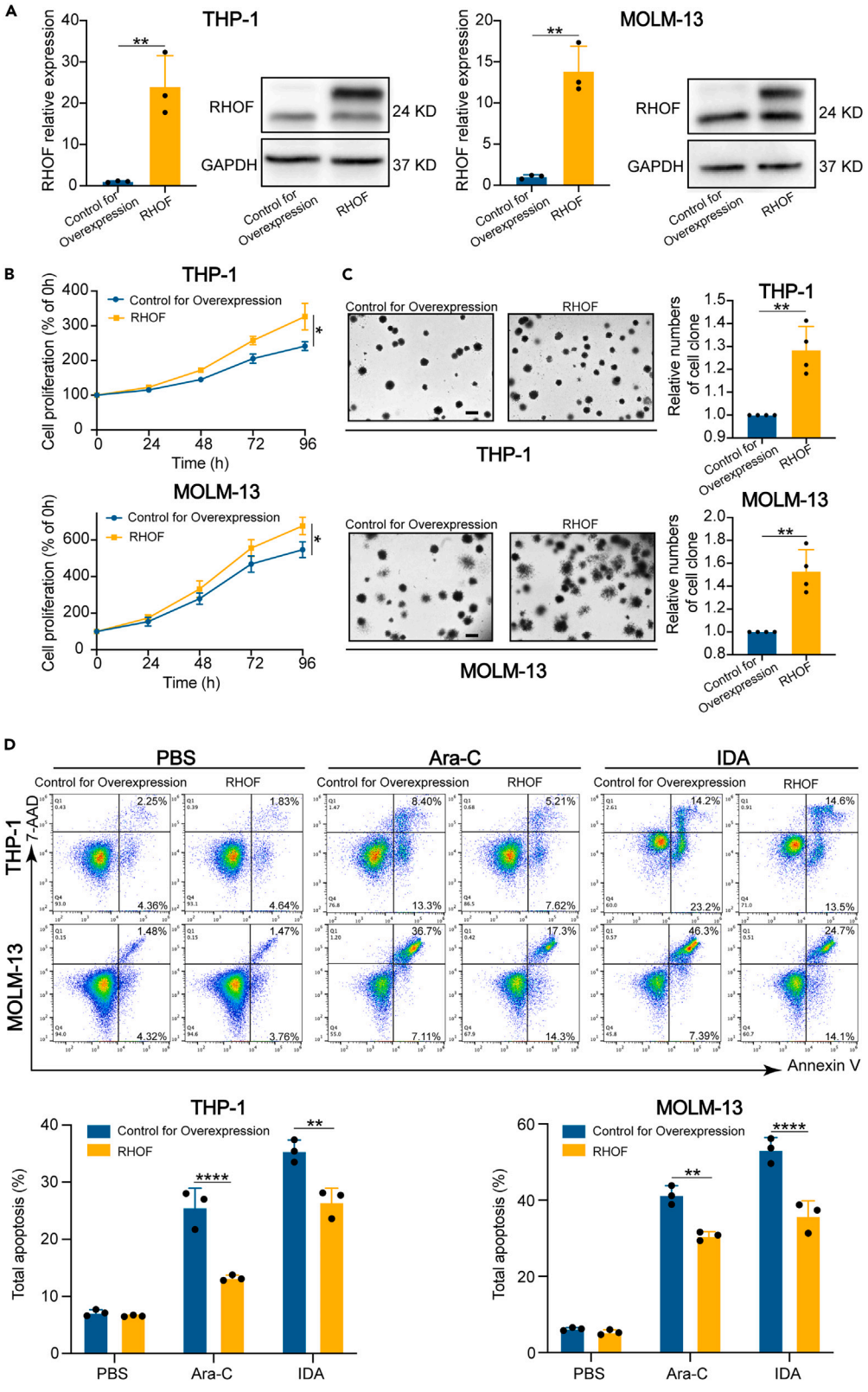
A
THP-1
RHOF relative expression
Control for Overexpression
RHOF
RHOF
GAPDH
24 KD
37 KD
MOLM-13
B
Cell proliferation (% of 0h)
Time (h)
C
Relative numbers of cell clone
D
PBS
Ara-C
IDA
7-AAD
Annexin V
Total apoptosis (%)

Figure 4. RHOF overexpression promotes cell growth and prevents chemotherapeutic-induced apoptosis

(A) Puromycin-selected Flag-tagged RHOF (RHOF) or control lentivirus (control for overexpression) was used to transfect THP-1 and MOLM-13 cells, which were subjected to RT-qPCR (n = 3) and western blotting.

(B) Proliferation of THP-1 and MOLM-13 cells (control for overexpression or RHOF) was determined by CCK-8 assays at 0, 24, 48, 72, and 96 h (n = 3).

(C) Colony formation assays (left). Scale bar: 500 μm. The statistical analysis is shown in the right panel (n = 4).

(D) THP-1 and MOLM-13 cells (control for overexpression or RHOF) were treated with 1.2 μM Ara-C and 0.03 μg/mL IDA for 48 h to measure apoptosis via flow cytometry (n = 3). Student's t tests were used for comparing two variables. One-way ANOVA test was used for multiple variable comparison. The data are presented as the means ± SD. *$p < 0.05$; **$p < 0.01$; ***$p < 0.001$.

($CD45^+$) in the bone marrow, peripheral blood, spleen, and liver significantly decreased in the RHOF-deficient group following chemotherapy. Additionally, hCD45 immunofluorescence staining of bone marrow sections revealed reduced infiltration of AML cells in the bone marrow after RHOF knockdown (Figure S2). Furthermore, the RHOF-deficient group exhibited a significant decrease in β-catenin expression in the bone marrow and liver following chemotherapy, as demonstrated by immunohistochemistry analysis (Figure 6F). Collectively, these findings suggest that downregulating RHOF expression can enhance the efficacy of chemotherapy.

XPO1 activates RHOF through direct protein interactions

To further investigate which molecules regulating RHOF in AML, we performed a comparative proteomic analysis of 293T cells overexpressing RHOF and control cells using liquid chromatography-mass spectrometry. As shown in Figure 7A, we analyzed various proteins that can interact with RHOF through mass spectrometry and identified exportin 1 (XPO1), a protein previously recognized for its significant role in AML.[41] XPO1, also known as chromosome region maintenance protein 1, plays a vital role in maintaining cellular homeostasis by regulating the export of a range of cargoes, including proteins and several RNAs, from the nucleus to the cytoplasm.[42] A colocalization study and a coimmunoprecipitation (coIP) analysis were performed to verify the protein-protein interaction between RHOF and XPO1. We found that RHOF colocalized with XPO1 in THP-1 and MOLM-13 cells expressing exogenous RHOF (Figure 7B). Furthermore, coIP experiments were conducted to confirm whether RHOF was directly associated with XPO1 in HEK293, THP-1, and MOLM-13 cells. Consistent with these findings, XPO1 was detected when RHOF was pulled down (Figure 7C). These findings confirmed that the RHOF protein can interact with XPO1. To further study the relationship between RHOF and XPO1, we detected XPO1 protein expression following RHOF knockdown or overexpression in the THP-1 and MOLM-13 cell lines and observed no obvious changes (Figure 7D). Interestingly, with prolonged treatment using the XPO1 inhibitor selinexor, we observed a gradual decrease in the expression of the RHOF protein, concurrent with an increase in cell apoptosis (Figures 7E and S3). Additionally, RHOF overexpression reduced the degree of apoptotic cell death induced by selinexor, as determined by staining with anti-annexin V and 7-aminoactinomycin D (Figure 7F). Interestingly, when comparing the expression levels of XPO1 in AML cells to those in normal control cells, we did not observe a significant increase, similar to the expression patterns of RHOF (Figures 1A and S4). This finding suggested that while XPO1 is an upstream regulator of RHOF, the overexpression of RHOF in AML may not solely depend on XPO1. Overall, these findings suggest that XPO1 can interact with RHOF through protein interactions and that the antileukemic effect of XPO1 inhibitors occurs partly through RHOF.

DISCUSSION

AML is the predominant manifestation of acute leukemia in the adult population. In the context of precision therapy, the primary obstacle lies in identifying therapeutic agents that specifically target AML. Presently, the treatment of AML relies heavily on the use of pantargeted drugs, which can be administered in conjunction with demethylating drugs, chemotherapeutic agents, or drugs that operate through alternative mechanisms. These treatment modalities represent a significant bottleneck within the realm of leukemia management. Consequently, there is an urgent need to identify novel therapeutic targets and diagnostic markers. In this study, we investigated the involvement of RHOF, a recently discovered Rho GTPase, in the development of AML and explored the underlying molecular mechanisms involved. RHOF could activate the AKT/β-catenin signaling pathway in AML cells, which may help explain its influence on stem cell characteristics such as clonogenicity and proliferation. In this study, we also explored the upstream regulators of RHOF and revealed that XPO1 can bind to RHOF in AML cells and modulate its downstream effects. Our findings demonstrate that targeting RHOF increases apoptosis in AML cells treated with chemotherapy agents, providing a foundation for further research into enhancing chemotherapy sensitivity through RHOF modulation. It is important to note, however, that while there is an interaction between RHOF and XPO1 and that inhibiting RHOF expression impacts the activation of the AKT/β-catenin pathway, more comprehensive experimental investigations are necessary to definitively establish these connections. This finding points to the need for continued research to fully elucidate the mechanisms by which RHOF influences chemotherapy responses and AML cell behavior. Furthermore, we provide evidence that inhibiting RHOF is an effective strategy for treating AML both *in vitro* and *in vivo*.

The role of small Rho GTPases in cancer has gained significant attention in recent years; however, their specific contribution to leukemia remains poorly understood. Several studies have reported aberrant transcription levels of *RHOBTB* genes in AML patients.[43] Moreover, low expression of RHOH contributes to chemotherapy resistance in leukemia cells.[44] In AML, high Cdc42 expression and activity are related to the transformation of hematopoietic stem cells into AML cells, which in turn prevents the differentiation of leukemic cells by controlling the symmetry of division.[45] Specifically, *RHOF* was found to be highly expressed in acute leukemia cell lines in a previous study,[46] but its detailed function in AML has not been determined. However, further research is needed to determine the clinical predictive significance of the RHOF. Here, suppressing RHOF was shown to enhance chemosensitivity by stimulating chemotherapy-triggered apoptosis *in vitro*.

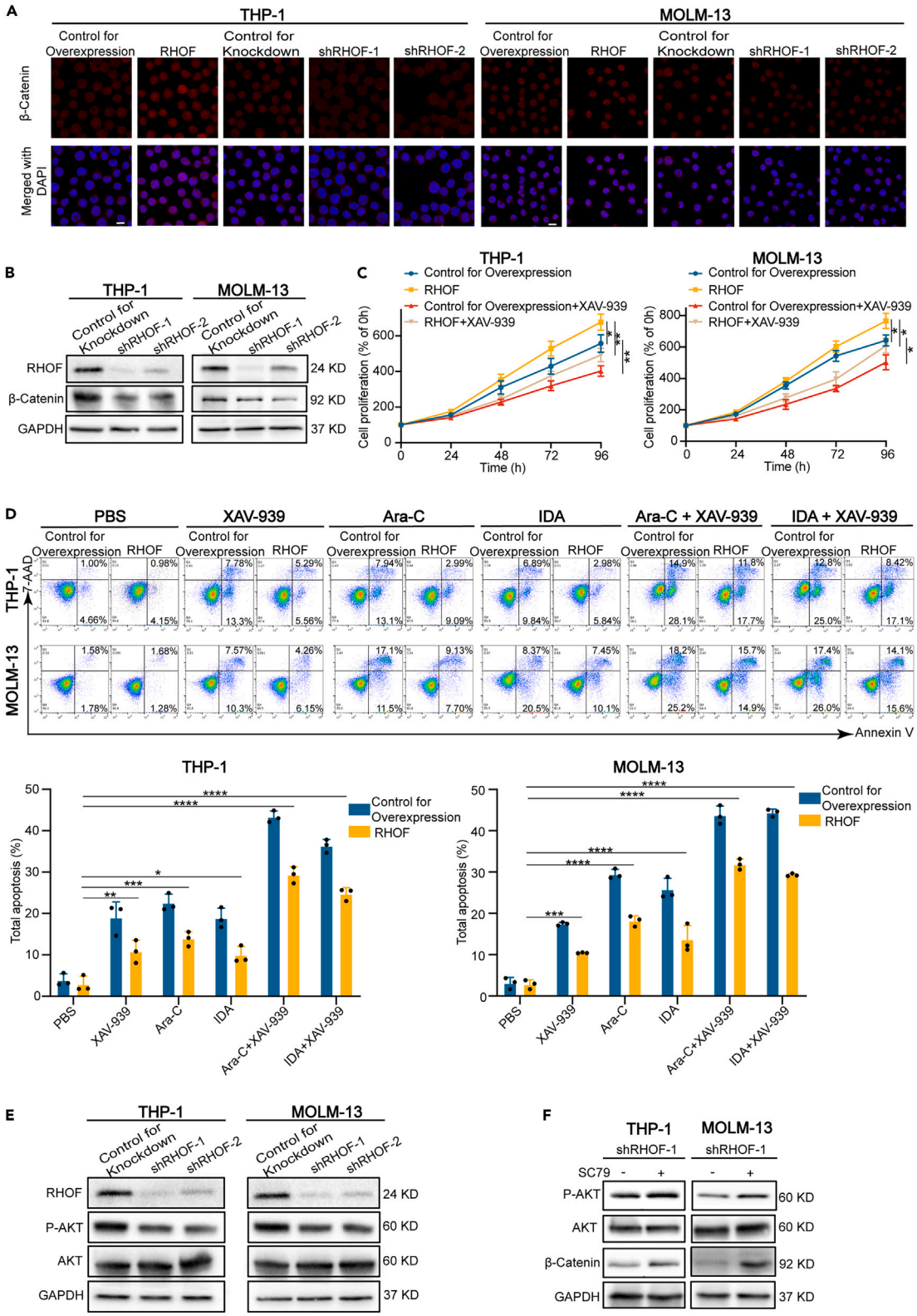
A
THP-1
MOLM-13
Control for Overexpression
RHOF
Control for Knockdown
shRHOF-1
shRHOF-2
β-Catenin
Merged with DAPI
B
THP-1
MOLM-13
RHOF
β-Catenin
GAPDH
24 KD
92 KD
37 KD
C
Control for Overexpression
RHOF
Control for Overexpression+XAV-939
RHOF+XAV-939
Cell proliferation (% of 0h)
Time (h)
D
PBS
XAV-939
Ara-C
IDA
Ara-C + XAV-939
IDA + XAV-939
7-AAD
Annexin V
Total apoptosis (%)
E
F
SC79
P-AKT
AKT
60 KD

Figure 5. RHOF augments AML proliferation via the AKT/β-catenin pathway

(A) To determine the localization and expression of β-catenin in THP-1 and MOLM-13 cells, immunofluorescence staining was performed with DAPI to stain the nucleus. DAPI (blue). β-Catenin (red). Scale bar: 10 μm.

(B) Western blot analysis of β-catenin proteins obtained from cells cultured with or without RHOF.

(C) A CCK-8 assay was performed to evaluate the effect of XAV-939 on the promotion of cell growth by RHOF-overexpressing cells (n = 3).

(D) The impact of XAV-939 on cell apoptosis or apoptosis induced by chemotherapeutics (1.0 μM Ara-C and 0.015 μg/mL IDA) was determined by flow cytometry in cells treated as described in (C) (n = 3).

(E) Western blot analysis was used to examine p-AKT activation in cells treated with or without RHOF.

(F) Cells with RHOF-suppressed cells were treated with an AKT agonist (10 μmol/L SC-79) for 24 h. Western blot analysis of β-catenin levels after activation of p-AKT. One-way ANOVA test was used for multiple variable comparison. The data are presented as the means ± SD. *$p < 0.05$; **$p < 0.01$; ***$p < 0.001$.

Furthermore, our *in vivo* experiments showed that mice harboring AML cells in which RHOF expression was knocked down exhibited decreased leukemic infiltration, demonstrating the therapeutic potential of targeting RHOF. In this study, RHOF demonstrates potential in modulating AML cell survival, curbing proliferation, and boosting sensitivity to chemotherapy. In conclusion, our findings suggest that RHOF could be a potential target, and further research is necessary to explore the combined suppression of RHOF and other substances to reduce AML chemoresistance.

The development of targeted therapies for AML will be greatly facilitated by understanding the functional mechanisms of RHOF. While it is well established that RHOF plays a role in negatively regulating apoptosis in malignancies, its functional mechanism varies depending on the cancer type and cellular context. Our research revealed a connection between RHOF and AKT, which was not previously known. In this study, we found that in AML, RHOF could modify AKT phosphorylation, which might play an important role in AML cell growth and apoptosis. Additionally, β-catenin was reported to be a core downstream protein in the canonical Wnt pathway.[47] The β-catenin protein is readily detected in primary AML samples and is required for the development of leukemia stem cells (LSCs) in AML.[48] The expression of β-catenin in AML cells predicts enhanced clonogenic capacity and poor prognosis.[49] Akt is recognized as an oncogene that possesses serine/threonine kinase activity and serves as an upstream regulator of β-catenin.[50] This regulatory role involves the stimulation of β-catenin nuclear translocation and activation, which is achieved either directly through β-catenin phosphorylation or indirectly through the phosphorylation and subsequent inactivation of GSK3β.[51,52] Specifically, the phosphorylation of β-catenin at Ser552 by Akt leads to protein stabilization, heightened nuclear accumulation, and augmented transcriptional activity.[53,54] Given the important role of the β-catenin signaling pathway in AML, our study provides insights into how RHOF promotes AML cell proliferation through Akt/β-catenin signaling.

We found increased expression of *RHOF* in patients with recurrent/refractory AML compared with patients with ND AML, suggesting a possible relationship between *RHOF* expression and the response to chemotherapy. Future studies on the clinical prognostic value of the RHOF are warranted. Interestingly, we subsequently identified a previously undescribed role for XPO1 in RHOF regulation. Involved in the transport of numerous proteins and RNAs with nuclear export signals, XPO1 is a significant nuclear export receptor that is mutated in various cancers. In AML, XPO1 is closely linked to unfavorable disease prognosis and resistance to chemotherapy.[55] In human cells, numerous tumor suppressor proteins have been identified as XPO1 substrates through proteomic research.[56–58] XPO1 inhibitors function primarily by retaining nuclei and activating important tumor suppressor proteins. Numerous preclinical studies have demonstrated that blocking nuclear export induces apoptosis and arrests the cell cycle in AML cells.[59,60] However, the exact mechanism by which XPO1 exerts its effect is not known. Here, we demonstrated that XPO1 interacts directly with RHOF, functioning as an upstream regulator of RHOF. Since the significance and role of XPO1 in AML remain unclear, future studies could help expand our understanding of the dysregulated molecular networks in AML.

This study provides the evidence that RHOF is involved in regulating apoptosis and drug resistance in AML. We experimentally demonstrated that RHOF activates the AKT/β-catenin signaling pathway, thereby accelerating the progression of AML. Additionally, we found that XPO1 can directly interact with RHOF, functioning as an upstream regulator of RHOF. Our research suggested that RHOF is a potential target for pathological research and targeted therapy for AML, as demonstrated by our *in vitro* and *in vivo* findings.

Limitations of the study

Although our research has elucidated the partial role of RHOF in leukemia and highlighted its potential as a therapeutic target, we acknowledge that there are limitations to our study that warrant further investigation in future research. First, the absence of an RHOF-specific inhibitor means that our findings rely on genetic methods to modulate RHOF expression, which do not directly simulate the effects of pharmacological inhibition and thus limit the immediate translational potential of our results. Additionally, the challenge of targeting Rho GTPases such as RHOF, which are notoriously difficult to inhibit due to their biochemical properties, further complicates the development of direct therapeutic interventions. Finally, this study was conducted using a limited number of AML cell lines and did not include patient-derived xenograft models or primary AML samples. This restricts our ability to generalize our findings across the heterogeneous landscape of AML and underscores the necessity of incorporating more diverse and clinically relevant models in future studies.

STAR★METHODS

Detailed methods are provided in the online version of this paper and include the following:

- KEY RESOURCES TABLE
- RESOURCE AVAILABILITY

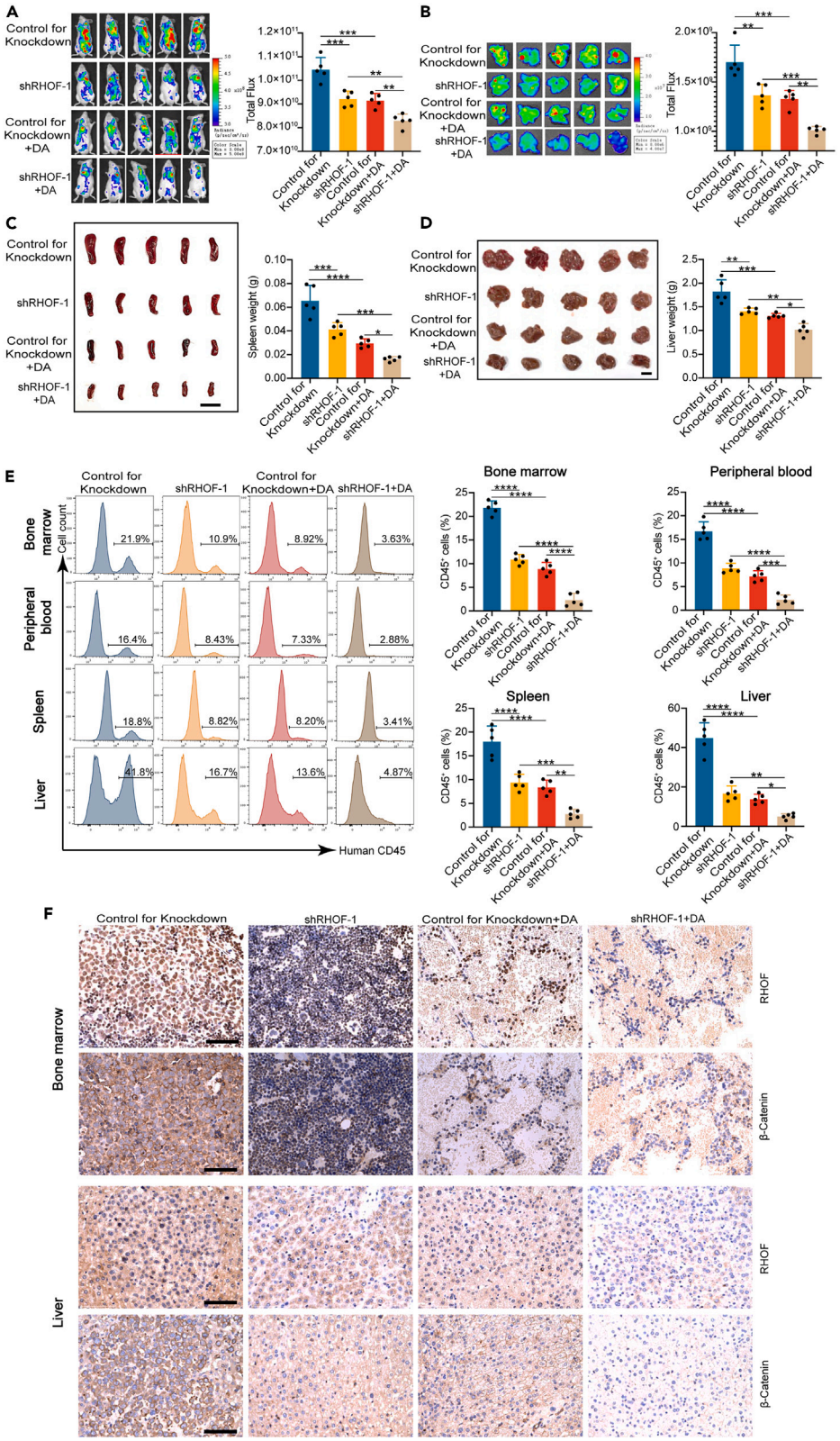
A
Control for Knockdown
shRHOF-1
Control for Knockdown +DA
shRHOF-1 +DA
Total Flux
B
C
Spleen weight (g)
D
Liver weight (g)
E
Bone marrow
Peripheral blood
Spleen
Liver
Cell count
Human CD45
CD45+ cells (%)
F
RHOF
β-Catenin

Figure 6. RHOF diminishes the responsiveness of AML cells to chemical drugs *in vivo*

(A) Detection of GFP signals *in vivo* using pseudocolor fluorescence intensity in mice transplanted with either control for knockdown or shRHOF-1-treated THP-1 cells followed by treatment with vehicle or chemotherapy ($n = 5$). The unit of radiance is photons/second/cm^2/steradian.

(B) Representative *in vivo* pseudocolor fluorescence intensity images of livers transplanted with control for knockdown or shRHOF-1 THP-1 cells followed by treatment with vehicle or chemotherapy ($n = 5$); the GFP signal was detected.

(C) Representative spleen images and weights of mice harboring THP-1 cells with or without RHOF expression followed by treatment with vehicle or chemotherapy ($n = 5$). Scale bar: 1 cm.

(D) Representative liver images and weights of mice bearing THP-1 cells with or without RHOF expression followed by treatment with vehicle or chemotherapy ($n = 5$). Scale bar: 1 cm.

(E) Human CD45$^+$ cells from the bone marrow, peripheral blood, spleen, and liver were analyzed via flow cytometry ($n = 5$).

(F) Representative immunohistochemical (IHC) images of bone marrow (BM) and liver specimens from the four groups demonstrating differences in RHOF and β-catenin expression. Scale bar: 75 μm. One-way ANOVA test was used for multiple variable comparison. The data are presented as the means ± SD. *$p < 0.05$; **$p < 0.01$; ***$p < 0.001$.

SUPPLEMENTAL INFORMATION

Supplemental information can be found online at https://doi.org/10.1016/j.isci.2024.110221.

ACKNOWLEDGMENTS

This work was supported by grants from the Distinguished Taishan Scholars in Climbing Plan (tspd20210321), the National Natural Science Foundation of China (82070160, 81700143, and 82000165), the Major Research Plan of the National Natural Science Foundation of China (91942306), the Key Program of Natural Science Foundation of Shandong Province (ZR2020KH016), the Fundamental Research Funds for the Central Universities (2022JC012), and the Independently Cultivate Innovative Teams of Jinan, Shandong Province (2021GXRC050).

AUTHOR CONTRIBUTIONS

X.W. and P.L. contributed equally to this study. P.L. and D.W. designed the research; X.W., Y.X., and W.L. performed the experiments; X.W., Y.M., and R.J. analyzed the data; X.W., P.L., and F.L. wrote the manuscript; X.W., W.L., J.Y., and Y.L. collected the clinical samples; G.L. and T.S. provided scientific and technical support; T.S., J.Y., F.L., and C.J. supervised and coordinated all aspects of the research. All authors revised, read, and approved the final manuscript.

DECLARATION OF INTERESTS

The authors declare no competing interests.

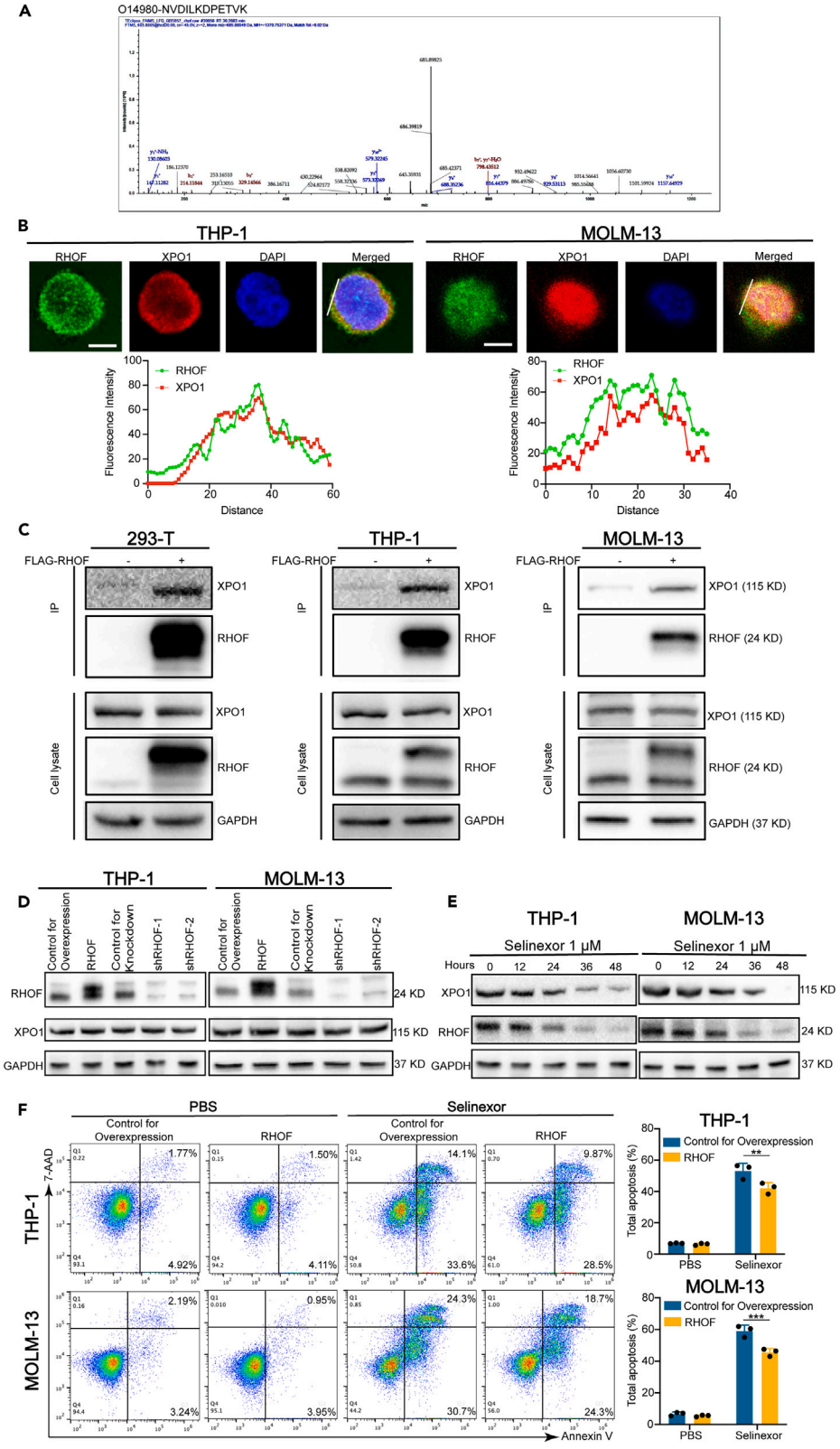
A
O14980-NVDILKDPETVK
B
THP-1
MOLM-13
RHOF
XPO1
DAPI
Merged
Fluorescence Intensity
Distance
C
293-T
THP-1
MOLM-13
FLAG-RHOF
IP
Cell lysate
XPO1
RHOF
GAPDH
XPO1 (115 KD)
RHOF (24 KD)
GAPDH (37 KD)
D
Control for Overexpression
RHOF
Control for Knockdown
shRHOF-1
shRHOF-2
24 KD
115 KD
37 KD
E
Selinexor 1 μM
Hours
0
12
24
36
48
F
PBS
Selinexor
7-AAD
Annexin V
1.77%
1.50%
14.1%
9.87%
4.92%
4.11%
33.6%
28.5%
2.19%
0.95%
24.3%
18.7%
3.24%
3.95%
30.7%
24.3%
Total apoptosis (%)
**
***

Figure 7. XPO1 activates RHOF through direct protein interactions

(A) Endogenous XPO1 protein was immunoprecipitated from HEK293 cells overexpressing RHOF. The tandem mass spectrometry spectrum of the XPO1 peptide is shown.

(B) Confocal double immunofluorescence analysis of THP-1 and MOLM-13 cells with anti-RHOF (green) and anti-XPO1 (red) antibodies. Scale bar: 10 μm. Fluorescence intensity tracking to provide a quantitative demonstration of the colocalization of XPO1 (red) and RHOF (green) in the lower panel.

(C) CoIP assay using either an RHOF antibody or an XPO1 antibody in 293T, THP-1, and MOLM-13 cells with or without exogenous RHOF expression.

(D) XPO1 protein expression following RHOF overexpression or knockdown in the THP-1 and MOLM-13 cell lines.

(E) Immunoblot showing the protein levels of RHOF in THP-1 and MOLM-13 cells treated with selinexor for the indicated durations.

(F) Flow cytometric analysis of the apoptosis of THP-1 and MOLM-13 cells (control for overexpression, RHOF) was carried out after the cells were sensitized for 48 h with selinexor (n = 3). One-way ANOVA test was used for multiple variable comparison. The data are presented as the means ± SD. *p < 0.05; **p < 0.01; ***p < 0.001.

Received: January 12, 2024
Revised: April 29, 2024
Accepted: June 5, 2024
Published: June 8, 2024

REFERENCES

1. De Kouchkovsky, I., and Abdul-Hay, M. (2016). Acute myeloid leukemia: a comprehensive review and 2016 update. Blood Cancer J. *6*, e441. https://doi.org/10.1038/bcj.2016.50.
2. Thol, F., and Ganser, A. (2020). Treatment of Relapsed Acute Myeloid Leukemia. Curr. Treat. Options Oncol. *21*, 66. https://doi.org/10.1007/s11864-020-00765-5.
3. Prada-Arismendy, J., Arroyave, J.C., and Röthlisberger, S. (2017). Molecular biomarkers in acute myeloid leukemia. Blood Rev. *31*, 63–76. https://doi.org/10.1016/j.blre.2016.08.005.
4. Medinger, M., Heim, D., Halter, J.P., Lengerke, C., and Passweg, J.R. (2019). [Diagnosis and Therapy of Acute Myeloid Leukemia]. Ther. Umsch. *76*, 481–486. https://doi.org/10.1024/0040-5930/a001126.
5. Chopra, M., and Bohlander, S.K. (2019). The cell of origin and the leukemia stem cell in acute myeloid leukemia. Genes Chromosomes Cancer *58*, 850–858. https://doi.org/10.1002/gcc.22805.
6. Wennerberg, K., Rossman, K.L., and Der, C.J. (2005). The Ras superfamily at a glance. J. Cell Sci. *118*, 843–846. https://doi.org/10.1242/jcs.01660.
7. Heasman, S.J., and Ridley, A.J. (2008). Mammalian Rho GTPases: new insights into their functions from in vivo studies. Nat. Rev. Mol. Cell Biol. *9*, 690–701. https://doi.org/10.1038/nrm2476.
8. van Helden, S.F.G., Anthony, E.C., Dee, R., and Hordijk, P.L. (2012). Rho GTPase expression in human myeloid cells. PLoS One *7*, e42563. https://doi.org/10.1371/journal.pone.0042563.
9. Buchsbaum, R.J. (2007). Rho activation at a glance. J. Cell Sci. *120*, 1149–1152. https://doi.org/10.1242/jcs.03428.
10. Schwartz, M. (2004). Rho signalling at a glance. J. Cell Sci. *117*, 5457–5458. https://doi.org/10.1242/jcs.01582.
11. Crosas-Molist, E., Samain, R., Kohlhammer, L., Orgaz, J.L., George, S.L., Maiques, O., Barcelo, J., and Sanz-Moreno, V. (2022). Rho GTPase signaling in cancer progression and dissemination. Physiol. Rev. *102*, 455–510. https://doi.org/10.1152/physrev.00045.2020.
12. Sahai, E., and Marshall, C.J. (2002). RHO-GTPases and cancer. Nat. Rev. Cancer *2*, 133–142. https://doi.org/10.1038/nrc725.
13. Toksoz, D., and Merdek, K.D. (2002). The Rho small GTPase: functions in health and disease. Histol. Histopathol. *17*, 915–927. https://doi.org/10.14670/HH-17.915.
14. Kakiuchi, M., Nishizawa, T., Ueda, H., Gotoh, K., Tanaka, A., Hayashi, A., Yamamoto, S., Tatsuno, K., Katoh, H., Watanabe, Y., et al. (2014). Recurrent gain-of-function mutations of RHOA in diffuse-type gastric carcinoma. Nat. Genet. *46*, 583–587. https://doi.org/10.1038/ng.2984.
15. Sakata-Yanagimoto, M., Enami, T., Yoshida, K., Shiraishi, Y., Ishii, R., Miyake, Y., Muto, H., Tsuyama, N., Sato-Otsubo, A., Okuno, Y., et al. (2014). Somatic RHOA mutation in angioimmunoblastic T cell lymphoma. Nat. Genet. *46*, 171–175. https://doi.org/10.1038/ng.2872.
16. Wang, K., Yuen, S.T., Xu, J., Lee, S.P., Yan, H.H.N., Shi, S.T., Siu, H.C., Deng, S., Chu, K.M., Law, S., et al. (2014). Whole-genome sequencing and comprehensive molecular profiling identify new driver mutations in gastric cancer. Nat. Genet. *46*, 573–582. https://doi.org/10.1038/ng.2983.
17. Yoo, H.Y., Sung, M.K., Lee, S.H., Kim, S., Lee, H., Park, S., Kim, S.C., Lee, B., Rho, K., Lee, J.E., et al. (2014). A recurrent inactivating mutation in RHOA GTPase in angioimmunoblastic T cell lymphoma. Nat. Genet. *46*, 371–375. https://doi.org/10.1038/ng.2916.
18. Zhou, J., Hayakawa, Y., Wang, T.C., and Bass, A.J. (2014). RhoA mutations identified in diffuse gastric cancer. Cancer Cell *26*, 9–11. https://doi.org/10.1016/j.ccr.2014.06.022.
19. Maldonado, M.D.M., and Dharmawardhane, S. (2018). Targeting Rac and Cdc42 GTPases in Cancer. Cancer Res. *78*, 3101–3111. https://doi.org/10.1158/0008-5472.CAN-18-0619.
20. King, S.J., Asokan, S.B., Haynes, E.M., Zimmerman, S.P., Rotty, J.D., Alb, J.G., Jr., Tagliatela, A., Blake, D.R., Lebedeva, I.P., Marston, D., et al. (2016). Lamellipodia are crucial for haptotactic sensing and response. J. Cell Sci. *129*, 2329–2342. https://doi.org/10.1242/jcs.184507.
21. Vu, H.L., Rosenbaum, S., Purwin, T.J., Davies, M.A., and Aplin, A.E. (2015). RAC1 P29S regulates PD-L1 expression in melanoma. Pigment Cell Melanoma Res. *28*, 590–598. https://doi.org/10.1111/pcmr.12392.
22. Bray, K., Gillette, M., Young, J., Loughran, E., Hwang, M., Sears, J.C., and Vargo-Gogola, T. (2013). Cdc42 overexpression induces hyperbranching in the developing mammary gland by enhancing cell migration. Breast Cancer Res. *15*, R91. https://doi.org/10.1186/bcr3487.
23. David, M.D., Petit, D., and Bertoglio, J. (2014). The RhoGAP ARHGAP19 controls cytokinesis and chromosome segregation in T lymphocytes. J. Cell Sci. *127*, 400–410. https://doi.org/10.1242/jcs.135079.
24. Florian, M.C., Dörr, K., Niebel, A., Daria, D., Schrezenmeier, H., Rojewski, M., Filippi, M.D., Hasenberg, A., Gunzer, M., Scharffetter-Kochanek, K., et al. (2012). Cdc42 activity regulates hematopoietic stem cell aging and rejuvenation. Cell Stem Cell *10*, 520–530. https://doi.org/10.1016/j.stem.2012.04.007.
25. Mulloy, J.C., Cancelas, J.A., Filippi, M.D., Kalfa, T.A., Guo, F., and Zheng, Y. (2010). Rho GTPases in hematopoiesis and hemopathies. Blood *115*, 936–947. https://doi.org/10.1182/blood-2009-09-198127.
26. Wang, L., Yang, L., Filippi, M.D., Williams, D.A., and Zheng, Y. (2006). Genetic deletion of Cdc42GAP reveals a role of Cdc42 in erythropoiesis and hematopoietic stem/progenitor cell survival, adhesion, and engraftment. Blood *107*, 98–105. https://doi.org/10.1182/blood-2005-05-2171.
27. Yang, L., Wang, L., Geiger, H., Cancelas, J.A., Mo, J., and Zheng, Y. (2007). Rho GTPase Cdc42 coordinates hematopoietic stem cell quiescence and niche interaction in the bone marrow. Proc. Natl. Acad. Sci. USA *104*, 5091–5096. https://doi.org/10.1073/pnas.0610819104.
28. Mele, S., Devereux, S., and Ridley, A.J. (2014). Rho and Rap guanosine triphosphatase signaling in B cells and chronic lymphocytic leukemia. Leuk. Lymphoma *55*, 1993–2001. https://doi.org/10.3109/10428194.2013.866666.
29. Kishimoto, M., Matsuda, T., Yanase, S., Katsumi, A., Suzuki, N., Ikejiri, M., Takagi, A., Ikawa, M., Kojima, T., Kunishima, S., et al. (2014). Rhof promotes murine marginal zone B cell development. Nagoya J. Med. Sci. *76*, 293–305.
30. Goh, W.I., Sudhaharan, T., Lim, K.B., Sem, K.P., Lau, C.L., and Ahmed, S. (2011). Rif-mDia1 interaction is involved in filopodium formation independent of Cdc42 and Rac

effectors. J. Biol. Chem. *286*, 13681–13694. https://doi.org/10.1074/jbc.M110.182683.
31. Pellegrin, S., and Mellor, H. (2005). The Rho family GTPase Rif induces filopodia through mDia2. Curr. Biol. *15*, 129–133. https://doi.org/10.1016/j.cub.2005.01.011.
32. Aspenstrom, P. (2014). Atypical Rho GTPases RhoD and Rif integrate cytoskeletal dynamics and membrane trafficking. Biol. Chem. *395*, 477–484. https://doi.org/10.1515/hsz-2013-0296.
33. Yang, R.M., Zhan, M., Xu, S.W., Long, M.M., Yang, L.H., Chen, W., Huang, S., Liu, Q., Zhou, J., Zhu, J., and Wang, J. (2017). miR-3656 expression enhances the chemosensitivity of pancreatic cancer to gemcitabine through modulation of the RHOF/EMT axis. Cell Death Dis. *8*, e3129. https://doi.org/10.1038/cddis.2017.530.
34. Shaverdashvili, K., Padlo, J., Weinblatt, D., Jia, Y., Jiang, W., Rao, D., Laczkó, D., Whelan, K.A., Lynch, J.P., Muir, A.B., and Katz, J.P. (2019). KLF4 activates NFκB signaling and esophageal epithelial inflammation via the Rho-related GTP-binding protein RHOF. PLoS One *14*, e0215746. https://doi.org/10.1371/journal.pone.0215746.
35. Li, S., Liu, Y., Bai, Y., Chen, M., Cheng, D., Wu, M., and Xia, J. (2021). Ras Homolog Family Member F, Filopodia Associated Promotes Hepatocellular Carcinoma Metastasis by Altering the Metabolic Status of Cancer Cells Through RAB3D. Hepatology *73*, 2361–2379. https://doi.org/10.1002/hep.31641.
36. Gouw, L.G., Reading, N.S., Jenson, S.D., Lim, M.S., and Elenitoba-Johnson, K.S.J. (2005). Expression of the Rho-family GTPase gene RHOF in lymphocyte subsets and malignant lymphomas. Br. J. Haematol. *129*, 531–533. https://doi.org/10.1111/j.1365-2141.2005.05481.x.
37. Luo, J., Chen, S., Chen, J., Zhou, Y., He, F., and Wang, E. (2022). Identification and validation of DNA methylation markers to predict axillary lymph node metastasis of breast cancer. PLoS One *17*, e0278270. https://doi.org/10.1371/journal.pone.0278270.
38. Wang, L., You, L.S., Ni, W.M., Ma, Q.L., Tong, Y., Mao, L.P., Qian, J.J., and Jin, J. (2013). β-Catenin and AKT are promising targets for combination therapy in acute myeloid leukemia. Leuk. Res. *37*, 1329–1340. https://doi.org/10.1016/j.leukres.2013.06.023.
39. Shahid, A.M., Um, I.H., Elshani, M., Zhang, Y., and Harrison, D.J. (2022). NUC-7738 regulates beta-catenin signalling resulting in reduced proliferation and self-renewal of AML cells. PLoS One *17*, e0278209. https://doi.org/10.1371/journal.pone.0278209.
40. Zhou, J., Toh, S.H.M., Chan, Z.L., Quah, J.Y., Chooi, J.Y., Tan, T.Z., Chong, P.S.Y., Zeng, Q., and Chng, W.J. (2018). A loss-of-function genetic screening reveals synergistic targeting of AKT/mTOR and WTN/β-catenin pathways for treatment of AML with high PRL-3 phosphatase. J. Hematol. Oncol. *11*, 36. https://doi.org/10.1186/s13045-018-0581-9.
41. Hing, Z.A., Fung, H.Y.J., Ranganathan, P., Mitchell, S., El-Gamal, D., Woyach, J.A., Williams, K., Goettl, V.M., Smith, J., Yu, X., et al. (2016). Next-generation XPO1 inhibitor shows improved efficacy and in vivo tolerability in hematological malignancies. Leukemia *30*, 2364–2372. https://doi.org/10.1038/leu.2016.136.
42. Azmi, A.S., Uddin, M.H., and Mohammad, R.M. (2021). Author Correction: The nuclear export protein XPO1 - from biology to targeted therapy, 10.1038/s41571-020-00442-4, 2020). Nat. Rev. Clin. Oncol. *18*, 190. https://doi.org/10.1038/s41571-020-00454-0.
43. Liu, P., Ma, Q., Chen, H., Zhang, L., and Zhang, X. (2021). Identification of RHOBTB2 aberration as an independent prognostic indicator in acute myeloid leukemia. Aging (Albany NY) *13*, 15269–15284. https://doi.org/10.18632/aging.203087.
44. Iwasaki, T., Katsumi, A., Kiyoi, H., Tanizaki, R., Ishikawa, Y., Ozeki, K., Kobayashi, M., Abe, A., Matsushita, T., Watanabe, T., et al. (2008). Prognostic implication and biological roles of RhoH in acute myeloid leukaemia. Eur. J. Haematol. *81*, 454–460. https://doi.org/10.1111/j.1600-0609.2008.01132.x.
45. Mizukawa, B., O'Brien, E., Moreira, D.C., Wunderlich, M., Hochstetler, C.L., Duan, X., Liu, W., Orr, E., Grimes, H.L., Mulloy, J.C., and Zheng, Y. (2017). The cell polarity determinant CDC42 controls division symmetry to block leukemia cell differentiation. Blood *130*, 1336–1346. https://doi.org/10.1182/blood-2016-12-758458.
46. Hou, Y., Zi, J., and Ge, Z. (2021). High Expression of RhoF Predicts Worse Overall Survival: A Potential Therapeutic Target for non-M3 Acute Myeloid Leukemia. J. Cancer *12*, 5530–5542. https://doi.org/10.7150/jca.52648.
47. Nusse, R., and Clevers, H. (2017). Wnt/β-Catenin Signaling, Disease, and Emerging Therapeutic Modalities. Cell *169*, 985–999. https://doi.org/10.1016/j.cell.2017.05.016.
48. Wang, Y., Krivtsov, A.V., Sinha, A.U., North, T.E., Goessling, W., Feng, Z., Zon, L.I., and Armstrong, S.A. (2010). The Wnt/beta-catenin pathway is required for the development of leukemia stem cells in AML. Science *327*, 1650–1653. https://doi.org/10.1126/science.1186624.
49. Ysebaert, L., Chicanne, G., Demur, C., De Toni, F., Prade-Houdellier, N., Ruidavets, J.B., Mansat-De Mas, V., Rigal-Huguet, F., Laurent, G., Payrastre, B., et al. (2006). Expression of beta-catenin by acute myeloid leukemia cells predicts enhanced clonogenic capacities and poor prognosis. Leukemia *20*, 1211–1216. https://doi.org/10.1038/sj.leu.2404239.
50. Hemmings, B.A. (1997). Akt signaling: linking membrane events to life and death decisions. Science *275*, 628–630. https://doi.org/10.1126/science.275.5300.628.
51. He, X.C., Yin, T., Grindley, J.C., Tian, Q., Sato, T., Tao, W.A., Dirisina, R., Porter-Westpfahl, K.S., Hembree, M., Johnson, T., et al. (2007). PTEN-deficient intestinal stem cells initiate intestinal polyposis. Nat. Genet. *39*, 189–198. https://doi.org/10.1038/ng1928.
52. Yost, C., Torres, M., Miller, J.R., Huang, E., Kimelman, D., and Moon, R.T. (1996). The axis-inducing activity, stability, and subcellular distribution of beta-catenin is regulated in Xenopus embryos by glycogen synthase kinase 3. Genes Dev. *10*, 1443–1454. https://doi.org/10.1101/gad.10.12.1443.
53. Taurin, S., Sandbo, N., Qin, Y., Browning, D., and Dulin, N.O. (2006). Phosphorylation of beta-catenin by cyclic AMP-dependent protein kinase. J. Biol. Chem. *281*, 9971–9976. https://doi.org/10.1074/jbc.M508778200.
54. Fang, D., Hawke, D., Zheng, Y., Xia, Y., Meisenhelder, J., Nika, H., Mills, G.B., Kobayashi, R., Hunter, T., and Lu, Z. (2007). Phosphorylation of beta-catenin by AKT promotes beta-catenin transcriptional activity. J. Biol. Chem. *282*, 11221–11229. https://doi.org/10.1074/jbc.M611871200.
55. Hutten, S., and Kehlenbach, R.H. (2007). CRM1-mediated nuclear export: to the pore and beyond. Trends Cell Biol. *17*, 193–201. https://doi.org/10.1016/j.tcb.2007.02.003.
56. Kojima, K., Kornblau, S.M., Ruvolo, V., Dilip, A., Duvvuri, S., Davis, R.E., Zhang, M., Wang, Z., Coombes, K.R., Zhang, N., et al. (2013). Prognostic impact and targeting of CRM1 in acute myeloid leukemia. Blood *121*, 4166–4174. https://doi.org/10.1182/blood-2012-08-447581.
57. Tan, D.S.P., Bedard, P.L., Kuruvilla, J., Siu, L.L., and Razak, A.R.A. (2014). Promising SINEs for embargoing nuclear-cytoplasmic export as an anticancer strategy. Cancer Discov. *4*, 527–537. https://doi.org/10.1158/2159-8290.CD-13-1005.
58. Taylor, J., Sendino, M., Gorelick, A.N., Pastore, A., Chang, M.T., Penson, A.V., Gavrila, E.I., Stewart, C., Melnik, E.M., Herrejon Chavez, F., et al. (2019). Altered Nuclear Export Signal Recognition as a Driver of Oncogenesis. Cancer Discov. *9*, 1452–1467. https://doi.org/10.1158/2159-8290.CD-19-0298.
59. Etchin, J., Sun, Q., Kentsis, A., Farmer, A., Zhang, Z.C., Sanda, T., Mansour, M.R., Barcelo, C., McCauley, D., Kauffman, M., et al. (2013). Antileukemic activity of nuclear export inhibitors that spare normal hematopoietic cells. Leukemia *27*, 66–74. https://doi.org/10.1038/leu.2012.219.
60. Ranganathan, P., Yu, X., Na, C., Santhanam, R., Shacham, S., Kauffman, M., Walker, A., Klisovic, R., Blum, W., Caligiuri, M., et al. (2012). Preclinical activity of a novel CRM1 inhibitor in acute myeloid leukemia. Blood *120*, 1765–1773. https://doi.org/10.1182/blood-2012-04-423160.
61. Schessl, C., Rawat, V.P.S., Cusan, M., Deshpande, A., Kohl, T.M., Rosten, P.M., Spiekermann, K., Humphries, R.K., Schnittger, S., Kern, W., et al. (2005). The AML1-ETO fusion gene and the FLT3 length mutation collaborate in inducing acute leukemia in mice. J. Clin. Invest. *115*, 2159–2168. https://doi.org/10.1172/JCI24225.
62. Sarry, J.E., Murphy, K., Perry, R., Sanchez, P.V., Secreto, A., Keefer, C., Swider, C.R., Strzelecki, A.C., Cavelier, C., Récher, C., et al. (2011). Human acute myelogenous leukemia stem cells are rare and heterogeneous when assayed in NOD/SCID/IL2Rγc-deficient mice. J. Clin. Invest. *121*, 384–395. https://doi.org/10.1172/JCI41495.

STAR★METHODS

KEY RESOURCES TABLE

REAGENT or RESOURCE	SOURCE	IDENTIFIER
Antibodies		
APC anti-human CD45 Antibody	Biolegend	Cat No: 304012 RRID: AB_314399
Mouse monoclonal anti-GAPDH	Share-bio	Cat No: SB-AB0038
Rabbit polyclonal anti-RHOF	Sino Biological	Cat No: 203681-T36
Mouse monoclonal anti-XPO1	Santa Cruz Biotechnology	Cat No: sc-74454 RRID: AB_1122704
Rabbit anti-Akt	Cell Signaling Technology	Cat No: 9272 RRID: AB_329827
Rabbit monoclonal anti-Phospho-Akt (Ser473)	Cell Signaling Technology	Cat No: 4060 RRID: AB_2315049
Rabbit monoclonal anti-β-Catenin	ABclonal Technology	Cat No: A19657 RRID: AB_2862719
Rabbit polyclonal anti-β-Catenin	abcam	Cat No: ab6302 RRID: AB_305407
Rabbit Polyclonal anti-RHOF	Proteintech	Cat No: 12290-1-AP RRID: AB_10644126
Rabbit monoclonal anti-CD45	abcam	Cat No: ab40763 RRID: AB_726545
Donkey anti-Rabbit IgG (H + L) Highly Cross-Adsorbed Secondary Antibody, Alexa Fluor™ 594	Thermo Fisher Scientific	Cat No: A21207 RRID: AB_141637
Donkey anti-Mouse IgG (H + L) Cross-Adsorbed Secondary Antibody, Alexa Fluor™ 594	Thermo Fisher Scientific	Cat No: A21203 RRID: AB_2535789
Donkey anti-Rabbit IgG (H + L) Highly Cross-Adsorbed Secondary Antibody, Alexa Fluor™ 647	Thermo Fisher Scientific	Cat No: A31573 RRID: AB_2536183
Anti-rabbit IgG, HRP-linked Antibody	Cell Signaling Technology	Cat No: 7074 RRID: AB_2099233
Anti-mouse IgG, HRP-linked Antibody	Cell Signaling Technology	Cat No: 7076 RRID: AB_330924
Cy3 conjugated Goat Anti-Rabbit IgG (H + L)	Servicebio	Cat No: GB21303 RRID: AB_2861435
Bacterial and virus strains		
GV493-hU6-MCS-CBh-gcGFP-IRES-puromycin	GeneChem, China	Cat No: GIEL0295808
pLV-hef1a-mNeongreen-P2A-Puro-WPRE-CMV-RHOF (Human, NM_019034)-3flag	Beijing Syngentech Co., LTD. (China)	Cat No: fw-4926
Biological samples		
bone marrow (BM) samples from AML patients	Qilu Hospital of Shandong University	N/A
Chemicals, peptides, and recombinant proteins		
XAV-939	MedChemExpress	Cat No: HY-15147
SKL2001	MedChemExpress	Cat No: HY-101085
Selinexor	Selleck	Cat No: S7252

(*Continued on next page*)

Continued

REAGENT or RESOURCE	SOURCE	IDENTIFIER
SC-79	MedChemExpress	Cat No: HY-18749
Ara-C	MedChemExpress	Cat No: HY-13605
DOX	GlpBio	Cat No: GC16994
IDA	MedChemExpress	Cat No: HY-17381A
Triton X-100	BioFroxx	Cat No: 1139
Puromycin	Sigma-Aldrich	Cat No: P8833
anti-Flag magnetic beads	MedChemExpress	Cat No: HY-K0207
TRIzol reagent	Takara	Cat No: 9108
Tween 20	Solarbio	Cat No: T8220
BSA	BioSharp	Cat No: BS114
Mounting Medium with DAPI	abcam	Cat No: Ab104139
ECL reagent	UU-Bio technology	Cat No: U10013
TBS	Servicebio	Cat No: G0001
DMSO	Solarbio	Cat No: D8371
4% Paraformaldehyde	Servicebio	Cat No: G1101
Protease inhibitor	Roche	Cat No: 4693159001
Phosphatase inhibitor	Roche	Cat No: 4906837001
primary antibody dilution	Biyuntian	Cat No: P0256
Critical commercial assays		
CD34 MicroBead Kit	Miltenyi Biotec	Cat No: 130-046-702
PrimeScript™ RT Master Mix	Takara	Cat No: RR036A
SYBR Green PCR kit	Takara	Cat No: RR820A
M-PER™ Mammalian Protein Extraction Reagent	Thermo Fisher	Cat No: 78501
Cell Counting Kit-8 kit	BestBio	Cat No: BB-4202
Annexin V/7-AAD apoptosis detection kit	BestBio	Cat No: BB-41012
Color PAGE Gel Rapid Preparation Kit (10%)	EpiZyme	Cat No: PG112
Color PAGE Gel Rapid Preparation Kit (12.5%)	EpiZyme	Cat No: PG113
BCA Protein Assay Kit	Biyuntian	Cat No: P0011
Rabbit two-step detection kit (rabbit enhanced polymer detection system)	Zhongshan Golden Bridge Biotechnology	Cat No: PV-9001
Deposited data		
Proteomic raw data	This paper	https://www.iprox.cn/page/PSV023.html;?url=1715230662321Ri6s, Password: KLjb
Experimental models: Cell lines		
THP-1	Hematology and Blood Diseases Hospital, Chinese Academy of Medical Sciences and Peking Union Medical College	N/A
MOLM-13	Hematology and Blood Diseases Hospital, Chinese Academy of Medical Sciences and Peking Union Medical College	N/A
HEK293T	Hematology and Blood Diseases Hospital, Chinese Academy of Medical Sciences and Peking Union Medical College	N/A
HS-5	High Magnetic Field Laboratory, Chinese Academy of Sciences	N/A

(*Continued on next page*)

Continued

REAGENT or RESOURCE	SOURCE	IDENTIFIER
Experimental models: Organisms/strains		
NOD-Prkdc^{scid}-Il2rg^{em1IDMO} (NSG) mice (male, 6 weeks old)	Beijing Vital River Laboratory Animal Technology Co., Ltd. (China)	N/A
Oligonucleotides		
shRNA targeting sequence 1: RHOF: 5′-ACGTCCTCATCAAGTGGTT-3′	GeneChem, China	N/A
shRNA targeting sequence 2: RHOF: 5′-CATCGGTGTTCGAGAAGTA-3′	GeneChem, China	N/A
RHOF, forward primer, 5′-CTCCTTCCCCGAGCACTACG-3′	Boshang Biological Technology Co., Ltd. (shanghai, China)	N/A
RHOF, reverse primer, 5′-TGTCGTAGCTGGTGGGATTC-3′	Boshang Biological Technology Co., Ltd. (shanghai, China)	N/A
GAPDH, forward primer, 5′- GGAGCGAGATCCCTCCAAAAT-3′	Boshang Biological Technology Co., Ltd. (shanghai, China)	N/A
GAPDH, Reverse primer, 5′- GGCTGTTGTCATACTTCTCATGG-3′	Boshang Biological Technology Co., Ltd. (shanghai, China)	N/A
Software and algorithms		
ImageJ software	National Institutes of Health	https://imagej.net/software/imagej/; RRID: SCR_003070
FlowJo software	FlowJo software	https://www.flowjo.com; RRID: SCR_008520
Living Image version 4.5 software	Living Image software	http://www.perkinelmer.com/catalog/category/id/living%20image%20software; RRID: SCR_014247
GraphPad Prism software	GraphPad Software	https://www.graphpad.com/scientific-software/prism/www.graphpad.com/scientific-software/prism/; RRID: SCR_002798
Adobe Illustrator	Adobe	https://www.adobe.com/; RRID: SCR_010279

RESOURCE AVAILABILITY

Lead contact

Further information and requests for resources and reagents should be directed to and will be fulfilled by the lead contact, Chunyan Ji (jichunyan@sdu.edu.cn).

Materials availability

This study did not generate new unique reagents. All materials used in this study were either commercially available or obtained through collaboration.

Data and code availability

The original Western blot images have been deposited in the supplemental materials. The proteomic raw data had been deposited to the iProX database with the the project ID: IPX0008768000 (https://www.iprox.cn/page/PSV023.html;?url=1715230662321Ri6s, Password: KLjb).

This paper does not report the original code.

Any additional information required to reanalyze the data reported in this paper is available from the lead contact upon request.

EXPERIMENTAL MODEL AND STUDY PARTICIPANT DETAILS

Cell lines and cell culture

The human leukemic cell lines THP-1 and MOLM-13 and human embryonic kidney 293T cells were obtained from the Institute of Hematology and Blood Diseases Hospital, Chinese Academy of Medical Sciences and Peking Union Medical College. The human BMSC line HS-5 was a gift from the High Magnetic Field Laboratory, Chinese Academy of Sciences. RPMI 1640 (Gibco, New York, USA, C11875500BT) medium was used to culture THP-1, MOLM-13 and HS-5 cells, while DMEM (Gibco, New York, USA, C11995500BT) was used to culture 293T cells

supplemented with 10% fetal bovine serum (Gibco, New York, USA, #10099-141) as well as penicillin and streptomycin (Invitrogen, Waltham, MA, USA, #15140122). We cultured all the cells in an incubator at 37°C and 5% CO_2. Short tandem repeat profiling was used to verify the identity and purity of the cell line on a regular basis. Shanghai Zhong Qiao Xin Zhou Biotechnology Co., Ltd., China, conducted the latest authentication of the cell lines. All the experiments were conducted using mycoplasma-free cells.

In vivo acute myeloid leukemia model

The animal experiments were carried out in accordance with institutional regulations and were approved by the Medical Ethics Committee of Shandong University (Approval Number: SDULCLL2020-2-12). The study adhered to the recommended ARRIVE guidelines. Male NOD-$Prkdc^{scid}$-$Il2rg^{em1IDMO}$ (NSG) mice aged 6 weeks were obtained from Beijing Vital River Laboratory Animal Technology Co., Ltd., China. The mice were intravenously injected with THP-1 cells. The cells were either transduced with a nontargeted short hairpin RNA (shRNA) serving as the control (THP-1 control for knockdown) or with RHOF shRNA (THP-1 shRHOF-1 and THP-1 shRHOF-2) at a concentration of 2×10^6 cells/100 μL. Each group consisted of four random mice. Mice were housed in a specific pathogen-free environment. We monitored the mice daily for signs of leukemia. We primarily assessed the incidence of AML in mouse models by observing clinical symptoms such as weight loss, a scruffy appearance, and a hunched posture. Additionally, we monitored the progression of AML by collecting blood samples from the tail vein and analyzing them for the presence of AML cells. When AML cells exceed 1% of nucleated cells in the peripheral blood, we consider the mouse to be in a state of AML disease.[61,62]

At 36 days after the AML model was established, GFP fluorescence was detected using an *in vivo* imaging system to quantify disease burden. The mice were sacrificed, and the peripheral blood, femurs, livers and spleens were collected and further analyzed. The presence of leukemia cells in the BM, peripheral blood, spleen, and liver was assessed using flow cytometry to detect human $CD45^+$ cells with an anti-hCD45-APC antibody (BioLegend, San Diego, CA, USA, #304012). In the BM, spleen and liver samples, hCD45 was detected by immunofluorescence. In addition, survival data were obtained ($n = 6$). The humane endpoints for euthanasia were based on criteria such as poor mobility, labored breathing, or a cumulative weight loss exceeding 20% of initial body weight. A Kaplan–Meier survival plot was used to display survival.

For the *in vivo* experiments shown in Figure 6, six-week-old male NSG mice were injected via the tail vein with two types of THP-1 cells (2×10^6 cells per mouse) that were transfected with viruses (THP-1-control for knockdown and THP-1-shRHOF-1 cells). On day 30 after cell injection, the treatment group received a daily dose of 50 mg/kg Ara-C (MedChemExpress, Monmouth Junction, NJ, USA, HY-13605) for 5 days with a daily dose of 1.5 mg/kg DOX (GlpBio, Montclair, CA, USA, GC16994) during the first 3 days intraperitoneally, and the control group was injected with PBS. The mice were divided into the following four subgroups: (i) Control for Knockdown, (ii) shRHOF-1, (iii) Control for Knockdown and DA, and (iv) shRHOF-1 and DA. An *in vivo* imaging system was used to quantitate disease burden and liver leukemia burden by detecting the GFP fluorescence signal. The livers and spleens of the mice were measured. BM cells, peripheral blood cells, spleen cells and liver cells were isolated and stained with anti-hCD45-APC (BioLegend, San Diego, CA, USA, #304012), and analyzed by flow cytometry (Gallios, Beckman Coulter, Brea, CA, USA). All the data were analyzed by using FlowJo 10.8.1. In the BM and liver samples, RHOF (1:100, Proteintech, Chicago, USA, 12290-1-AP) and β-catenin (1:2000, Abcam, Cambridge, MA, USA, ab6302) were detected by immunohistochemistry.

Patient samples

In this study, we included a total of 76 patients with AML, aged 15–81 years, with no restriction on gender, ancestry, race or ethnicity or socioeconomic information. All patients were recruited from Qilu Hospital of Shandong University to obtain BM samples. AML patients at various stages, such as those with ND AML ($n = 31$), relapsed/refractory AML ($n = 25$) and CR ($n = 20$), were subjected to sample collection. Mononuclear cells were isolated and used for RT−qPCR analysis. Six patients (3 patients with ND AML and 3 patients who achieved CR) were subjected to both WB analysis and qPCR analysis. $CD34^+$ cells were isolated from 3 patients with ND AML via CD34 MicroBeads (Miltenyi Biotec, Bergisch Gladbach, Germany, #130-046-702) according to the manufacturer's instructions for WB analysis. The Declaration of Helsinki was followed to obtain informed consent. All laboratory experiments were approved by the Medical Ethics Committee of Qilu Hospital using primary samples (Approval Number: KYLL-202206-016).

METHOD DETAILS

Chemical inhibitors and agonists

We dissolved the β-catenin inhibitor XAV-939 (MedChemExpress, Monmouth Junction, NJ, USA, HY-15147) in dimethyl sulfoxide (DMSO, Solarbio, Beijing, China, D8371) and added it to the cell culture medium to culture the cells at a final concentration of 10 μM. The β-catenin agonist SKL2001 (MedChemExpress, Monmouth Junction, NJ, USA, HY-101085) was dissolved in DMSO and added to the cell culture medium to culture the cells at a final concentration of 5 μM. In this study, DMSO was used to dissolve the XPO1 inhibitor selinexor (Selleck, Huston, TX, USA, S7252), which was added to the cell culture medium at final concentrations of 1 μM and 2 μM in culture. The AKT agonist SC-79 (MedChemExpress, Monmouth Junction, NJ, USA, HY-18749) was dissolved in DMSO (10 μM in culture medium).

Lentiviral transduction

We generated lentiviral constructs designed to suppress RHOF expression from GeneChem (Shanghai, China). Additionally, a lentivirus expressing RHOF with a FLAG tag was purchased from Beijing Syngentech Co., Ltd. (China). The vectors used were GV493-hU6-MCS-CBh-gcGFP-IRES-puromycin and pLV-hef1a-mNeongreen-P2A-Puro-WPRE-CMV-RHOF (human, NM_019034)-3flag. For the lentivirus infection

process, shRHOF (GeneChem, China, NM_019034, Gene ID:54509) and concentrated RHOF virus were directly added to the cells. After 48 h of lentivirus exposure, the transduced cells were selected with 1 μg/mL puromycin (Sigma–Aldrich, St. Louis, MO, USA, P8833) to ensure successful transduction.

Quantitative reverse transcription PCR (RT–qPCR)

Total RNA was extracted from cells using TRIzol reagent (Takara, Shiga, Japan, #9108). This RNA was then reverse-transcribed into cDNA using PrimeScript RT Master Mix (Takara, Shiga, Japan, RR036A). For real-time PCR analysis, the SYBR Green gene expression assay (Takara, Shiga, Japan, RR820A) was performed on a Roche Applied Science LightCycler 480 II Real-Time PCR System. The relative expression levels of mRNA were quantified using the 2^(-ΔΔCT) method, with *GAPDH* serving as the internal control.

Western blot

M-PER Mammalian Protein Extraction Reagent (Thermo Fisher, Waltham, MA, USA, #78501) with a protease inhibitor (Roche, Basel, Switzerland, #4693159001) and phosphatase inhibitor (Roche, Basel, Switzerland, #4906837001) was used to lyse the cells. Then, the protein concentration was quantified by using a BCA protein assay kit (Biyuntian, Shanghai, China, P0011). We separated the proteins using 10% or 12.5% SDS–PAGE (EpiZyme, Shanghai, China, PG112 and PG113) and electrotransferred them onto PVDF membranes (Millipore, MA, USA, IPVH00010). 5% bovine serum albumin (BSA, BioSharp, Hefei, China, BS114) was used to block the membranes at room temperature for 1 h. The membranes were incubated overnight at 4°C on a plate shaker with primary antibody dilution (Biyuntian, Shanghai, China, P0256) diluted with the following primary antibodies: anti-GAPDH (1:2000, Share-bio, Shanghai, China, SB-AB0038), anti-RHOF (1:1000, Sino Biological, Beijing, China, #203681-T36), anti-XPO1 (1:1000, Santa Cruz Biotechnology, Santa Cruz, CA, USA, sc-74454), anti-AKT (1:1000, Cell Signaling Technology, MA, USA, #9272), anti-*p*-AKT (1:1000, Cell Signaling Technology, MA, USA, #4060), and anti-β-catenin (1:1000, ABclonal Technology, Wuhan, China, A19657). For secondary antibodies (1:3000, CST, MA, USA, #7074, #7076), 1 h of incubation at room temperature was used. The protein bands were visualized using a SageCapture chemiluminescent imaging system (ChampChemi 610 Plus, Beijing, China).

Proliferation analysis

The proliferation of THP-1 and MOLM-13 cells was assessed by seeding them at densities of 4×10^3 cells per well and 5×10^3 cells per well, respectively, in 96-well plates. The plates were cultured at 37°C in an incubator. Over the next four days, each well was treated with 10 μL of CCK-8 reagent (BestBio, Shanghai, China, BB-4202) and incubated for 4 h. The optical density was then measured at 450 nm and 630 nm using a microplate reader (HIMFD, Biotek, Winooski, VT, USA) to assess cell proliferation.

Colony formation assay

For the colony formation assay, 800 cells per well were seeded into 24-well plates containing 1 mL of methylcellulose medium (MethoCult H4230, Stem Cell Technologies, Vancouver, Canada, #04230). The plates were then incubated at 37°C in a humidified environment. After 14 days, colony formation was examined under a microscope (BZ-X800LE, Keyence, Osaka, Japan). The number of colonies was quantified using ImageJ software to analyze the number of clusters formed.

Apoptosis analysis

For apoptosis analysis, cells were treated with 1.2 μM cytarabine (Ara-C, MedChemExpress, Monmouth Junction, NJ, USA, HY-13605) or 0.03 μg/mL IDA (MedChemExpress, Monmouth Junction, NJ, USA, HY-17381A) for 48 h. Following treatment, 5×10^5 cells per well in 6-well plates were stained using an Annexin V/7-AAD apoptosis detection kit (BestBio, Shanghai, China, BB-41012). Apoptosis was then assessed by flow cytometry using a Gallios machine (Beckman Coulter, Brea, CA, USA).

Protein immunoprecipitation (IP) assays

For the protein immunoprecipitation (IP) assays, lysates were prepared from 293T cells using lysis buffer. The lysates were then incubated with anti-Flag magnetic beads (MedChemExpress, Monmouth Junction, NJ, USA, HY-K0207) for 16 h at 4°C with rotation. After incubation, the beads, which contained affinity-bound proteins, were washed three times with immunoprecipitation wash buffer (TBST: 50 mM Tris-HCl, 150 mM NaCl, 0.5% Tween 20, pH 7.4). The immunoprecipitates were finally eluted with sample buffer in 1× SDS–PAGE loading buffer and subsequently analyzed by Western blotting. The gels were then digested for mass spectrometry-based sequencing (Beijing Qinglian Biotech Co., Ltd., China). Briefly, spectra were acquired using an Orbitrap ECLIPSE Mass Spectrometer (ThermoFisher Scientific). MS1 spectra were obtained at a resolution of 120,000, with a scan range from 350 to 2000 m/z, a normalized AGC target set to standard, and a maximum injection time (IT) of 50 ms. MS1 precursors selected for MS2 analysis had an intensity greater than 5.0e3, a charge state between 2 and 6, and met a precursor envelope fit threshold of 30% within a 1.2 m/z fit window. For MS2 analysis, ions were isolated in the quadrupole with a 1.2 m/z window, collected to a normalized AGC target of 5.0e4 or a maximum IT of 22 ms, fragmented with a normalized HCD collision energy of 30, and the resulting spectra were acquired at a resolution of 15,000, with a first mass of 110 m/z.

Coimmunoprecipitation (Co-IP)

Anti-Flag magnetic beads (MedChemExpress, Monmouth Junction, NJ, USA, HY-K0207) were incubated with the entire protein mixture for 16 h at 4°C with rotation. After incubation, the bead-antibody-antigen complexes were washed three times with immunoprecipitation wash buffer to remove unbound proteins. The bound proteins were then detected using Western blotting. For this purpose, we used an anti-RHOF antibody (1:1000, Sino Biological, Beijing, China, 203681-T36) and an anti-XPO1 antibody (1:1000, Santa Cruz Biotechnology, Santa Cruz, CA, USA, sc-74454) to identify the proteins of interest captured by the beads.

Immunofluorescence

After fixation in 4% formaldehyde (Servicebio, Wuhan, China, G1101), BM, spleen, and liver tissues were embedded in paraffin and sectioned. The sections underwent dewaxing and rehydration followed by antigen retrieval. Subsequently, the slides were labeled with hCD45 antibody (1:100, Abcam, Cambridge, MA, USA, ab40763) and incubated overnight at 4°C. The next day, the slides were incubated with a secondary antibody (Servicebio, Wuhan, China, GB21303) at room temperature for 1 h. The stained sections were then examined using a laser scanning confocal microscope (LSM980, Zeiss, Germany).

Colocalization assay

THP-1 or MOLM-13 cells were transfected with an RHOF plasmid for 24 h, after which they were harvested for immunofluorescence analysis. The cells were incubated with rabbit-derived anti-RHOF antibody (1:100, Proteintech, Chicago, USA, 12290-1-AP) and mouse-derived anti-XPO1 antibody (1:100, Santa Cruz Biotechnology, Santa Cruz, CA, USA, sc-74454) for 16 h at 4°C. Next, the cells were incubated with the following fluorescently labeled secondary antibodies: donkey anti-mouse IgG (H + L) Alexa 594 (1:2000, Thermo Fisher, Waltham, MA, USA, A21203) and donkey anti-rabbit IgG (H + L) Alexa 647 (1:2000, Thermo Fisher, Waltham, MA, USA, A31573) for 1 h. Finally, the cells were examined under a laser scanning confocal microscope (LSM980, Zeiss, Germany).

Immunohistochemistry (IHC) analysis

After fixation in 4% formaldehyde (Servicebio, Wuhan, China, G1101), BM and liver tissues were embedded in paraffin and sectioned. The sections were then dewaxed and rehydrated, followed by antigen retrieval. Subsequently, the sections were labeled with RHOF antibody (1:100, Proteintech, Chicago, USA, 12290-1-AP) and β-catenin antibody (1:2000, Abcam, Cambridge, MA, USA, ab6302) overnight at 4°C. The sections were then incubated with a secondary antibody (goat anti-rabbit IgG, Zhongshan Golden Bridge Biotechnology, Beijing, China, PV-9001 kit) at room temperature for 20 min, following the instructions provided with the kit. The stained sections were examined under an EVOS FL Auto 2 microscope (Thermo Fisher Scientific, Waltham, MA, USA).

Live animal imaging

Mice were anesthetized using isoflurane (RWD, Shenzhen, China) gas anesthesia. Live animal imaging was subsequently performed with an *in vivo* imaging system (IVIS Spectrum, PerkinElmer, USA). The imaging results were analyzed using Living Image software (version 4.5). To ensure the comparability of the results, all mice in the same experiment were imaged under uniform parameters.

QUANTIFICATION AND STATISTICAL ANALYSIS

All data were analyzed using GraphPad Prism 8.0. The mean ± standard deviation (SD) is shown. An unpaired Student's t test was utilized to analyze differences between two groups. For normally distributed data, one-way ANOVA followed by Tukey test was used to analyze differences between more than 2 groups. For variables with skewed distributions and unequal variances, a nonparametric Kruskal–Walli test was used. K–M survival analyses were performed with the log rank test. p values less than 0.05 indicated statistical significance.